Progress in Nuclear Energy, Vol. 17, No. 3, pp. 303–335, 1986.
Printed in Great Britain.

0149–1970/86 $0.00+.50

ASSEMBLY HOMOGENIZATION TECHNIQUES FOR LIGHT WATER REACTOR ANALYSIS

K. S. SMITH

Studsvik of America, 1087 Beacon Street, Suite 301, Newton, Massachusetts 02159, U.S.A.

(*Received* 14 *November* 1985)

Abstract—Recent progress in development and application of advanced assembly homogenization methods for light water reactor analysis is reviewed. Practical difficulties arising from conventional flux-weighting approximations are discussed and numerical examples given. The mathematical foundations for homogenization methods are outlined. Two methods, Equivalence Theory and Generalized Equivalence Theory which are theoretically capable of eliminating homogenization error are reviewed. Practical means of obtaining approximate homogenized parameters are presented and numerical examples are used to contrast the two methods.

Applications of these techniques to PWR baffle/reflector homogenization and BWR bundle homogenization are discussed. Nodal solutions to realistic reactor problems are compared to fine-mesh PDQ calculations, and the accuracy of the advanced homogenization methods is established. Remaining problem areas are investigated, and directions for future research are suggested.

1. INTRODUCTION

The physics design and analysis of modern light water reactors necessitates extensive knowledge of quantities which influence reactor operation. The determination of power distributions, control rod worths, shutdown margins, and isotopic depletion rates must be known throughout the reactor cycle. The ability to perform such core-follow calculations depends critically on models employed to predict the free neutron density in space, direction and energy. If thermal-hydraulic properties of the reactor and fundamental nuclear data are assumed to be known, the reactor physicist is faced with the conceptually straightforward task of solving the three-dimensional neutron transport equation.[1] Unfortunately the complexity inherent in explicit modeling of every fuel pin, control rod, burnable poison rod, and water channel limits the direct methods of solving the three-dimensional transport equation. Although tools such as three-dimensional continuous energy Monte Carlo are available,[2] the magnitude of the computational problem posed by explicit modeling is such that even the most sophisticated digital computers are incapable of determining reactor parameters, with the possible exception of k_{eff}, to the required degree of accuracy. Deterministic neutron transport methods (e.g. multigroup S_N^3, integral transport,[4,5] or collision probability[6] methods) are similarly overwhelmed by the complexity of the computational problem of explicit geometrical modeling on a core-wide basis.

1.1. *Spatial homogenization and group condensation*

Many reactor analysis methods[4–8] circumvent the computational burden of explicit geometrical modeling by coupling geometrically-simple, energy-intensive calculations with few-group, geometrically-complicated calculations via spatial homogenization and group condensation. Typically, pin cell transport spectral calculations (whose geometry consists of fuel pin, clad, coolant, and buffer material) are performed in 1-dimensional cylindrical geometry with 20–100 energy groups. The resultant neutron spectrum is used to collapse cross sections to 6–20 groups. Collapsed pin cell cross sections are used in assembly transport calculations which model all fuel pins, control rods, water channels, can walls, etc. Assembly calculations can be performed by employing one of two distinct methods: (i) collision probability methods[8] which explicitly model all fuel pins and channels, or (ii) Cartesian geometry transport calculations (including collision probability[6], transmission probability,[5] S_N^3, or nodal transport[7,9,10] methods) in which pin cell cross sections are homogenized into 'equivalent' cross sections. It is important that the assembly transport calculation be performed with sufficient numbers of

energy groups to account properly for the spectral interactions between pins of different compositions, between pins and control rods, between control rods and water channel, etc. It is also important to recognize that approximations are required to define the 'equivalent' pin cell cross sections; simply flux-volume weighting of cross sections is not sufficiently accurate. Other approximations such as the SPH,[11] CPH,[7] and g-factor[5] methods have been developed to perform the pin cell homogenization, but they will not be treated in this paper. The details of the lattice calculation, although outside the scope of this paper, are very important, particularly since lattice calculations must be performed (for each type of fuel assembly) for several fuel temperatures, moderator temperatures, moderator densities (void fractions), boron concentrations, and depletion steps. For our purposes, it will be assumed that a lattice physics code, such as CASMO,[6] DIT,[4] EPRI-CELL,[12] MULTI-MEDIUM,[7] TGBLA,[13] or WIMS,[8] is available to the reactor physicist. The goal of this paper is to examine theoretical foundations for and practical application of three-dimensional reactor analysis methods which utilize information from lattice physics calculations.

1.2. *Global heterogeneous reactor analysis methods*

The lattice physics calculations described in Section 1.1 provide an abundance of information with respect to spatial and spectral distributions of reaction rates and neutron densities. The question of how to make the best use of this information has prompted several different approaches to reactor analysis. The two most distinctly different approaches are the 'pin-by-pin' and the 'nodal' diffusion methods.

In a 'pin-by-pin' diffusion method, cross sections utilized in the lattice physics calculation are group collapsed (usually to 2–4 groups) on a pin-by-pin basis. Straightforward spectral collapse of pin cell cross sections for use in diffusion theory models will not preserve the properties of the lattice physics solution. Consequently, adjustments to absorption cross sections or diffusion coefficients are made such that diffusion calculations will preserve certain region-averaged interaction rates.[4,6,8] Although this adjustment procedure is not rigorous, for reasons to be discussed presently, adjusted cross sections can be obtained such that fine-mesh diffusion calculations do accurately predict the lattice reaction rate distributions. Full two-dimensional, planar, pin-by-pin diffusion calculations are then performed (with codes such as PDQ[14]) using the collapsed, and adjusted, pin cell cross sections. The drawbacks to fine-mesh diffusion calculations arise primarily from the fact that the large expense of the detailed calculations restrict their use to a single 'representative' plane. The three distinct advantages of these models (explicit assembly-to-assembly interaction, automated pin power peaking, and explicit pin depletion capabilities) are severely limited by the fact that details of axial variations in control rod positions, moderator density (void fraction) and depletion must be represented in the calculation of a single representative plane. These limitations are much more pronounced in BWR analyses than in PWR analyses because of the large axial variations in void fractions and the extensive use of control rods during BWR cycles.

1.3. *Nodal reactor analysis methods*

Alternative methods which provide true three-dimensional reactor analysis capabilities have been developed over the years, and most of these methods fall into a general class called nodal diffusion methods. Although early nodal methods[15,16] were based on ad-hoc approximations or heuristic derivations, many consistently-formulated nodal methods have been developed during the 1970s. These advanced nodal methods have been proven to be capable of solving the three-dimensional neutron diffusion equation, using assembly-size mesh, with calculational error in assembly-averaged powers of less than 2%. A companion paper[9] by R. D. Lawrence contains an excellent review of these important methods. Most of these nodal methods assume that the pin-by-pin lattice cross sections have been spatially homogenized to obtain 'equivalent' diffusion theory parameters which are spatially constant (or smoothly varying) over the entire cross sectional area of a fuel assembly. Provided accurate homogenized parameters can be determined, modern nodal codes are capable of accurately predicting global reactor power shapes, critical control rod patterns, boron letdown curves, etc. In addition to these global parameters, it is necessary that the local pin peaking and nonuniform assembly depletion can be modeled by the nodal methods. The difficulty in predicting peak pin powers arises from the fact that the nodal solution provides only nodal (volume-averaged) and surface (face-averaged) fluxes and reaction rates. Three quite different approaches to reconstructing intra-assembly heterogeneities have been developed. The first approach is simply to modulate the smooth nodal flux shapes with the detailed assembly flux shapes (obtained from lattice physics codes). Such approaches are straightforward and quite inexpensive, but not accurate in regions of the core where adjacent assemblies are very different in enrichment or

depletion.[17] A second approach is to perform imbedded heterogeneous calculations for a single-assembly (or small groups of assemblies), using boundary conditions obtained from the nodal solution.[18,19] These approaches are quite accurate, rather expensive and generally restricted to two-dimensional geometry. A third approach to flux reconstruction is to modulate assembly flux shapes with nonseparable (polynomial) flux shapes whose coefficients are determined by forcing the nonseparable shapes to match volume-averaged, surface-averaged, and corner point fluxes obtained from nodal codes.[19–26] The interpolation of corner point fluxes requires the introduction of additional approximations, although the interpolation can be performed using information provided by nodal codes and basic cross section data.[19,20,23] This approach has been shown to be quite inexpensive and is comparable in accuracy to detailed pin-by-pin models.[19]

It is important that nodal solutions account for nonuniform depletion effects so that the basic nodal-averaged quantities, and the resulting reconstructed flux shapes, will be accurately predicted. Depletion effects have been examined, and it has been shown that assembly-averaged powers can be in error 10% or more when depletion is assumed to be uniform within a PWR assembly.[27,28] Consequently, most nodal depletions are performed with a 2×2 spatial mesh in each PWR assembly. The use of this finer spatial mesh is easily accomplished but costly, and it undermines the fact that nodal methods are capable of solving the diffusion equation with nonuniform cross sections while retaining an assembly-size mesh. Wagner[27,28] has successfully demonstrated that nonuniform depletion effects can be accounted for by representing the burnup dependence of the cross section with separable (along each coordinate axis) quadratic polynomials.

These recent advancements in nodal method theory have improved nodal reactor analysis to the point that accurate three-dimensional nodal depletion calculations which allow the determination of local pin power peaking can be performed routinely and economically. These developments have advanced nodal methods to the point where nodal analysis is capable of replacing detailed pin-by-pin calculations, providing that accurate 'equivalent' homogenized reactor parameters can be determined. It is thus important that accurate methods for homogenizing reactor assemblies be developed and employed. The major portion of this paper is devoted to the discussion of advanced techniques for performing assembly homogenization. Specifically, inter-assembly transport effects and the impact of homogenization approximations will be examined. Recently developed homogenization techniques will be discussed and applied to realistic benchmark problems, giving special emphasis to PWR baffle/reflector homogenization.

2. HOMOGENIZATION THEORY

2.1. *Homogenization theory*

One of the simplest means of demonstrating the difficulties associated with spatial homogenization is to postulate that an exact solution to the multigroup neutron transport equation is known for a truly heterogeneous reactor. That is, the solution to the equation

$$\nabla \cdot \mathbf{J}_g(\mathbf{r}) + \Sigma_{tg}(\mathbf{r})\Phi_g(\mathbf{r}) = \sum_{g'=1}^{G} [1/k_{\text{eff}} M_{gg'}(\mathbf{r}) + \Sigma_{gg'}(\mathbf{r})]\Phi_{g'}(\mathbf{r}), \quad (1)$$

where

$$\mathbf{J}_g(\mathbf{r}) \equiv \int d\boldsymbol{\Omega}\, \boldsymbol{\Omega} \cdot \boldsymbol{\Phi}_g(\mathbf{r}, \boldsymbol{\Omega}),$$

$$\Phi_g(\mathbf{r}) = \int d\boldsymbol{\Omega}\, \boldsymbol{\Phi}_g(\mathbf{r}, \boldsymbol{\Omega}),$$

$$M_{gg'}(\mathbf{r}) = \chi_g \nu \Sigma_{fg'}(\mathbf{r}),$$

$$\Sigma_{gg'}(\mathbf{r}) = \tfrac{1}{2} \int d\mu_0 \Sigma_{gg'}(\mathbf{r}, \mu_0); \quad \mu_0 = \boldsymbol{\Omega} \cdot \boldsymbol{\Omega}',$$

$$k_{\text{eff}} = \text{reactor eigenvalue},$$

where $\boldsymbol{\Phi}_g(\mathbf{r}, \boldsymbol{\Omega})$ is the group g directional flux density, G is the number of energy groups, and the cross section notation is quite standard.

The first step in defining homogenized parameters is to choose those heterogeneous reactor properties which should be reproduced when the homogenized problem is solved. The homogenization process itself makes it difficult (if not impossible) to preserve quantities which characterize any particular subregion within a homogenized region, and one generally settles for the preservation of the spatial integrals (over each homogenized region) of the quantities of interest. The three quantities of most importance are the node-averaged group reaction rates, the surface-averaged group currents, and the reactor eigenvalue. Writing an equation analogous to equation (1) for the homogenized model of the reactor as:

$$\nabla \cdot \hat{\mathbf{J}}_g(\mathbf{r}) + \hat{\Sigma}_{tg}(\mathbf{r})\hat{\Phi}_g(\mathbf{r}) = \sum_{g'=1}^{G} [1/k_{\text{eff}} \hat{M}_{gg'}(\mathbf{r}) + \hat{\Sigma}_{gg'}(\mathbf{r})]\hat{\Phi}_{g'}(\mathbf{r}), \quad (2)$$

makes it clear that the homogenized parameters must obey the relationships

$$\int_{V_i} \hat{\Sigma}_{\alpha g}(\mathbf{r})\hat{\Phi}_g(\mathbf{r})\,d\mathbf{r} = \int_{V_i} \Sigma_{\alpha g}(\mathbf{r})\,\Phi_g(\mathbf{r})\,d\mathbf{r}, \qquad (3)$$

$$g = 1, 2 \ldots G$$
$$\alpha = t, gg', \text{etc.}$$

and

$$\int_{S_i^k} \nabla \cdot \hat{\mathbf{J}}_g(\mathbf{r}) \cdot d\mathbf{S} = \int_{S_i^k} \nabla \cdot \mathbf{J}_g(\mathbf{r}) \cdot d\mathbf{S}, \qquad (4)$$

where S_i^k is the k^{th} surface of homogenized region i and V_i is the volume of homogenized region i. If all homogenized parameters are assumed to be spatially constant within each node, the 'ideal' homogenized parameters can be defined rigorously by

$$\hat{\Sigma}_{\alpha g}^i \equiv \frac{\int_{V_i} \Sigma_{\alpha g}(\mathbf{r})\Phi_g(\mathbf{r})\,d\mathbf{r}}{\int_{V_i} \hat{\Phi}_g(\mathbf{r})\,d\mathbf{r}}. \qquad (5)$$

Equation (5) simply states that the heterogeneous cross sections should be flux-volume weighted to yield the desired parameters. Evaluation of equation (4) depends on the form of the neutron transport operator used in the homogenized reactor model. In the usual case in which the diffusion approximation is used, that is

$$\hat{\mathbf{J}}_g(\mathbf{r}) = -\hat{D}_g(\mathbf{r})\nabla\hat{\Phi}_g(\mathbf{r}),$$

equation (4) dictates that

$$\hat{D}_g^i \equiv \frac{-\int_{S_i^k} \mathbf{J}_g(\mathbf{r}) \cdot d\mathbf{S}}{\int_{S_i^k} \nabla\hat{\Phi}_g(\mathbf{r}) \cdot d\mathbf{S}}. \qquad (6)$$

Close examination of equations (5) and (6) reveals the practical difficulty in evaluating the homogenized parameters. The heterogeneous reactor solution must be known *a priori*, as must the solution to the homogenized diffusion problem which requires definition of the homogenized parameters. Since the homogenized flux is strongly coupled to the values of the homogenized parameters, a nonlinearity is introduced into the evaluation process. An additional dilemma exists in that the relationship expressed by equation (6) must be valid for all of the k surfaces of each homogenized node. If conventional continuity of scalar flux and net current are imposed on all nodal surfaces, equation (6) will define values of D_g^i which are different on each surface of the homogenized node. It is thus impossible to define *spatially constant* values of D_g^i which preserve all of the quantities of equations (3) and (4). Consequently, this situation dictates that either additional degrees of freedom be added to the homogenized parameters which allow the conditions of equations (3) and (4) to be met, or that some of the constraints be relaxed.

2.2. *Conventional homogenization methods*

The most commonly employed procedures for determining homogenized parameters relax some of the constraints mentioned in the preceding section and focus strictly on the preservation of reaction rates.[5,6,8] Typically, $\Phi_g(\mathbf{r})$ is approximated by solving a 2-dimensional lattice physics problem for each different type of assembly imposing $\mathbf{J}_g \cdot n = 0$ (zero net current) boundary conditions. At this level, all of the heterogeneous details of the assembly are either directly or indirectly represented, and all transport effects are modeled. Only the boundary conditions are approximate. Homogenized parameters are then found by using the assembly heterogeneous flux, $\Phi_{Ag}(\mathbf{r})$, in the numerator of equation (5). In addition, the denominator of equation (5) is replaced by the corresponding heterogeneous integral:

$$\int \hat{\Phi}_g(\mathbf{r})\,d\mathbf{r} = \int \Phi_{Ag}(\mathbf{r})\,d\mathbf{r}. \qquad (7)$$

This relationship, although plausible, is not automatically satisfied since none of the homogenized regions in the heterogeneous reactor satisfies the assumed zero net current boundary conditions used in the assembly homogenization calculation.

The last, and perhaps most inaccurate, approximation that is frequently made is that the homogenized diffusion coefficient can be defined such that

$$\hat{D}_g^i = \frac{\int_{V_i} D_g(\mathbf{r})\Phi_{Ag}(\mathbf{r})\,d\mathbf{r}}{\int_{V_i} \Phi_{Ag}(\mathbf{r})\,d\mathbf{r}}. \qquad (8)$$

Homogenized parameters which are determined by making the previous three assumptions are referred to, here, as assembly homogenized cross sections (AXSs). These constants are routinely used in the analysis of power reactors. In a rigorous sense, the solution to a global homogenized reactor problem will preserve none of the quantities (reaction rates) of equation (3). The argument that AXSs will preserve the reaction rates of the heterogeneous reactor is based on the fact that they do preserve the reaction rates of the infinite lattice. In a reactor having finite boundaries or multiple assembly types, however, reaction rates will not be preserved. The reactor analyst's ultimate decision of whether or not to use flux-weighted parameters should be based on a practical understanding of the error which results from their use and on an understanding of practical alternatives.

Utilization of numerical benchmarks which do not involve homogenization approximations is a desirable means of evaluating the magnitude of error introduced by assembly homogenization methods. Many such problems have been developed and several realistic problems will be employed in this paper to evaluate the accuracy of different homogenization methods. These

benchmark problems are fully specified by geometric descriptions of fuel assemblies, the distribution of assemblies throughout the reactor, and cross sections of the constituent materials. Since this paper is emphasizing spatial homogenization (and not spectral collapsing approximations, cross section specification is given in the form of two-group macroscopic cross sections. Heterogeneous 'reference' solutions can therefore be found by solving the neutron transport equation with full geometric detail. Solutions to the analogous homogenized reactor problem can then be compared to the reference solutions, thus the accuracy of the homogenization methods can be ascertained. Reference solutions employed in this paper have been generated using the QUANTM[29] code which solves the two-group P_N equations in x–y geometry by using the analytic nodal[30,31] (spatial) and the simplified P_N[32] (angular) approximation. It will therefore be assumed that homogenized pin cell cross sections are known for each of the heterogeneous regions (fuel pins, control rods, burnable poison rods, etc.). These benchmark problems avoid ambiguities which arise from fundamental cross section data, resonance treatments, or pin cell homogenizations, and allow direct testing of assembly homogenization approximations.

2.3. *Homogenization error in the HAFAS BWR benchmark problem*[33]

Homogenization approximations in BWRs can give rise to significant error. The sizable error can be attributed to a number of phenomena including (i) the presence of sizable water gaps between fuel assemblies, (ii) the use of enrichment zoning and burnable absorber pins within assemblies, (iii) the presence of control blades during much of the operating cycle, and (iv) the large variations in the water density (void fraction) throughout the core. The HAFAS BWR benchmark problem, described in Appendix 1.4, models control blades, narrow and wide water gaps, fresh and depleted fuel assemblies, void distributions, and provides a stringent test of homogenization methods. The HAFAS problem has a simplified assembly layout in which fuel pins are modeled using three different fuel enrichments. A reference solution to the transport version (isotropic scattering, $\Sigma_{tr,g} = 1/3D_g$) of the HAFAS problem was obtained using the QUANTM code with 49 nodes per assembly and the $P3$ option. Assembly calculations were performed for each fuel assembly type using the same spatial and angular approximations of QUANTM. AXSs were computed for each assembly type and the global reactor power distribution was computed using one-node-per-assembly spatial mesh and P_1 (diffusion theory) angular approximation in QUANTM. This solution is identical to the solution obtained by the QUANDRY nodal diffusion code since the mathematical approximations are identical. The homogenized diffusion solution to the HAFAS problem is compared with the reference transport solution in Table 1.

A complete map of the reference power distribution and the error in the homogenized diffusion solution is displayed in Fig. 1. Error of the magnitude demonstrated in Table 1 is not uncommon in nodal BWR analysis. Nodal diffusion models make many implicit assumptions and it is of interest to examine the contribution of each assumption to the total error.

2.3.1. *Reflector albedo error.* Nodal simulators[15,34,35] frequently rely on the use of empirically-determined albedos to model the reflector. Such albedos are, at best, only approximate. In the nodal solutions obtained for use in this paper, however, the reflector is explicitly modeled. Hence, albedos are eliminated from consideration as a source of the error since the benchmark reference solution and the homogenized solution employ the same geometrical and cross section representation for the reflector.

2.3.2. *Spatial truncation error.* Nodal simulators introduce an additional problem by providing only approximate solutions to the homogenized diffusion equation. Spatial truncation must be considered as a source of error in the homogenized nodal solutions. The magnitude of spatial truncation error depends strongly on the nodal method which is employed and on the spatial mesh that is used within each fuel assembly. In fact, many nodal methods (e.g. PRESTO,[34] SIMULATE,[35] EPRI NODEP,[36] etc.)

Table 1. Results for the homogenized HAFAS BWR problem using AXSs

Quantity	Error in homogenized solution
k_{eff}	−0.44%
Average error in assembly power	+5.5%
Maximum error in assembly power	+12.8%
Maximum error in Group 1 assembly absorption rate	+7.3%
Maximum error in Group 1 assembly fission rate	+8.9%
Maximum error in Group 1 assembly removal rate	+7.0%
Maximum error in Group 2 assembly absorption rate	+12.3%
Maximum error in Group 2 assembly fission rate	+13.7%

will not yield the correct solution to the diffusion equation for any mesh spacing. For modern, consistently formulated nodal methods,[9] such as the Analytic Nodal Method,[30,31] it is well known that the error in assembly powers obtained by using an assembly-sized spatial mesh in QUANTM are at most of the order of 1–2%. A one-eighth core, four-mesh-per-assembly QUANTM solution to the HAFAS problem was computed and is compared to the reference solution in Fig. 1. The largest deviation from the one-mesh-per-assembly solution can be seen to be only a few tenths of a percent. The spatial truncation error in the one-mesh-per assembly QUANTM solution to the HAFAS BWR problem is therefore negligible and not a major contributor to the error in the homogenized diffusion equation.

2.3.3. *Inter-assembly transport effects.* It has been proposed that the homogenized transport equation, rather than the diffusion equation, should be solved in order to obtain the best estimate of the reactor power distribution; isolated assembly calculations which are used in assembly homogenization have ignored all inter-assembly transport effects. In order to determine the magnitude of these effects, a QUANTM *P*3 transport solution to the homogenized transport equation was computed using nine meshes per assembly. The transport solution is compared to the reference heterogeneous and homogenized diffusion solution in Fig. 1. The transport solution displays a 1.5–3.0% increase in assembly powers at the core periphery. Assemblies which surround the control rods are predicted to have approximately 1.0% lower powers in the transport solution. The net effect of using transport theory rather than diffusion theory is a radial power tilt of about 3.0%. This demonstrates that inter-assembly transport effects in the homogenized problem are small, and it is therefore not the use of diffusion theory which leads to the large error in the nodal model of the HAFAS BWR problem.

2.3.4. *Error from assembly homogenization boundary conditions.* The boundary conditions used in the assembly transport calculations, from which homogenized cross sections are obtained, are another potential source of homogenization error. One could argue

Reference Heterogeneous *P*3 Solution					1.095	0.690	0.399
Error in *P*1 AXS Solution 1×1 Mesh					7.0%	8.3%	12.8%
Error in *P*1 AXS Solution 3×3 Mesh					7.0%	8.2%	12.8%
Error in *P*3 AXS Solution 3×3 Mesh					8.8%	9.8%	15.7%
				1.478	1.204	0.996	0.513
				3.0%	4.0%	5.8%	7.7%
				3.0%	3.9%	5.6%	7.7%
				4.1%	5.0%	7.4%	9.6%
			0.995	1.277	1.370	0.978	0.641
			10.9%	−1.0%	3.5%	3.3%	8.0%
			11.0%	−1.2%	3.4%	3.2%	8.0%
			10.3%	−0.7%	4.5%	4.4%	9.9%
		1.122	0.888	1.268	1.100	1.018	0.572
		4.4%	6.7%	−4.0%	−1.0%	2.2%	5.3%
		4.6%	6.7%	−4.0%	−1.1%	2.2%	5.2%
		3.0%	5.4%	−3.6%	−0.5%	3.5%	6.7%
	1.591	1.502	1.382	0.811	0.764	0.798	0.590
	−5.3%	−7.6%	−7.6%	4.0%	11.7%	−1.7%	4.8%
	−5.2%	−7.7%	−7.5%	4.0%	11.9%	−1.8%	4.8%
	−6.0%	−8.5%	−7.9%	2.9%	11.4%	−1.0%	6.4%
1.609	1.432	1.675	1.238	0.857	0.650	0.839	0.512
−4.1%	−6.2%	−6.7%	8.7%	5.1%	9.9%	−1.8%	2.4%
−4.0%	−6.1%	−6.7%	−8.8%	5.2%	9.9%	−1.8%	2.4%
−5.1%	−7.2%	−7.4%	−9.5%	4.0%	9.0%	−0.8%	3.7%
1.371	1.197	1.265	1.051	0.943	1.024	1.050	0.807	0.569
−3.9%	−4.8%	−6.9%	3.1%	7.1%	−7.9%	−4.0%	−2.5%	2.6%
−3.8%	−4.7%	−6.8%	3.2%	7.2%	−8.0%	−4.0%	−2.4%	2.7%
−5.2%	−6.2%	−8.1%	1.0%	5.5%	−8.4%	−3.6%	−1.7%	4.2%

Fig. 1. AXS assembly power distribution for the HAFAS BWR problem.

that the use of k_{eff} or buckling searches to force criticality in the assembly calculations distorts the spatial and spectral shapes of the reaction rates. This argument is certainly valid since neither the use of k_{eff} or buckling searches is capable of modeling assembly leakage which is a surface phenomenon. It is important, however, to understand the magnitude of the error which is introduced by such approximations. There exist many nonlinear iteration schemes[18] in which buckling values or assembly surface boundary conditions are obtained from conventional homogenized diffusion solutions to the reactor model. Assembly calculations can then be recomputed using the local boundary conditions, and homogenized cross sections can then be computed using the improved assembly flux distribution. These approaches result in improved homogenized parameters by nonlinear iteration between nodal reactor and assembly calculations. Such nonlinear 'rehomogenization' strategies are cumbersome, and some insight must be used to avoid recomputation of assembly calculations for every different assembly. In the case of the HAFAS benchmark problem, such issues can be addressed by a much more direct approach—using the 'exact' core-wide reference flux distributions to spatially collapse cross sections for each individual assembly. Reference homogenized cross sections (RXSs) obtained in this manner are entirely equivalent to a case in which assembly calculations are recomputed for every assembly in the reactor with rigorous boundary conditions and exact leakage rates. Results for the HAFAS BWR problem obtained using RXSs are compared to the reference and AXS solutions in Fig. 2 and are summarized in Table 2.

The results obtained using RXSs are clearly improved at the core periphery, though very large error exists throughout much of the remainder of the core. Comparisons of the actual values of the cross

Reference Heterogeneous *P*3 Solution Error in *P*1 AXS Solution 1 × 1 Mesh Error in *P*1 AXS Solution 1 × 1 Mesh					1.095 7.0% 3.0%	0.690 8.3% 4.4%	0.399 12.8% 4.9%
				1.478 3.0% 1.2%	1.204 4.0% 1.9%	0.996 5.8% 3.2%	0.513 7.7% 3.1%
			0.995 10.9% 11.2%	1.277 −1.0% −1.3%	1.370 3.5% 1.4%	0.978 3.3% 1.5%	0.641 8.0% 2.8%
		1.122 4.4% 7.8%	0.888 6.7% 8.4%	1.268 −4.0% −3.8%	1.100 −1.0% −1.8%	1.018 2.2% 0.1%	0.572 5.3% 1.2%
	1.591 −5.3% −3.5%	1.502 −7.6% −4.5%	1.382 −7.6% −5.6%	0.811 4.0% 6.4%	0.764 11.7% 10.9%	0.798 −1.7% −2.5%	0.590 4.8% 0.5%
1.609 −4.1% −2.1%	1.432 −6.2% −3.9%	1.675 −6.7% −4.1%	1.238 −8.7% −6.3%	0.857 −5.1% −6.9%	0.650 9.9% 9.2%	0.839 −1.8% −3.3%	0.512 2.4% 1.1%
1.371 −3.9% −2.3%	1.197 −4.8% −2.8%	1.265 −6.9% −4.8%	1.051 −3.1% −7.2%	0.943 7.1% 8.3%	1.024 −7.9% −6.4%	1.050 −4.0% −4.6%	0.807 −2.5% −3.4%	0.569 2.6% 1.4%

Fig. 2. RXS assembly power distribution for the HAFAS BWR problem.

Table 2. Results for the homogenized HAFAS BWR problem using RXSs

Quantity	Error in homogenized solution	
	AXS solution	RXS solution
k_{eff}	−0.44%	−0.34%
Average error in assembly power	5.5%	4.1%
Maximum error in assembly power	+12.8%	+11.2%

sections between the reference homogenized cross sections and the AXSs reveal that the most significant changes are 2.0–5.0% lower thermal absorption and fission cross sections in the peripheral bundle RXSs and a 2.0–3.0% lower thermal absorption and fission cross sections in the rodded bundle RXSs. Although these cross section differences are significant, the large error which exists in a nodal solution which used 'exact' flux-weighted cross sections clearly demonstrates that inaccuracies in nodal solutions cannot be overcome by employing more accurate boundary conditions for the determination of assembly homogenized parameters. Moreover, any rehomogenization technique which relies simply on a more accurate determination of cross sections will not alleviate the large homogenization error that are common in nodal BWR analyses.

The insight that has been gained from the examination of the HAFAS BWR problem suggests that the following phenomena are *not* responsible for the large error present in nodal reactor analyses:

inaccurate albedo values used to model reflector effects

inaccurate nodal diffusion solution methods

inter-assembly transport effects

boundary conditions used in assembly homogenization

inaccurate homogenized cross sections.

3. ADVANCED HOMOGENIZATION METHODS

3.1. *Introduction*

The persistence of large error in the solution to the homogenized diffusion equation even when exact flux-weighted cross sections are used indicates that the inaccurate approximation of the leakage terms [equation (4)] in the node-integrated diffusion equation are a major contributor to the error. The use of conventional spatially-constant diffusion coefficients (computed by flux-volume weighting $\Sigma_{tr}(r)$, flux-weighting $1/\Sigma_{tr}(r)$, or any other spatial weighting technique) does not directly address the issue of preservation of surface integrated currents and cannot be expected to preserve the properties of a heterogeneous reactor. Many novel homogenization methods[37–42] have been developed, some of which attempt to preserve nodal leakage rates. In one-dimensional geometry, it is possible to determine diffusion coefficients (and cross sections) which preserve surface currents when the preservation of reaction rates is relaxed so that only group-summed reaction rates are preserved.[1] These techniques have not been successfully extended to the multi-dimensional case. A number of homogenization techniques determine diffusion coefficients by matching certain components of heterogeneous response matrix elements.[43,44] Although such methods have better mathematical basis than conventional flux weighting techniques, they have not found widespread application because of the computational burden of calculating the required response matrix elements instead of the standard single-assembly homogenization calculation. The difficulty of determining the appropriate values for homogenized diffusion coefficients is, perhaps, best illustrated by considering a hypothetical one-dimensional reactor, for which a 1-group heterogeneous flux distribution is assumed to have been computed. Consider two adjacent nodes extracted from this reactor as depicted in Fig. 3(a). 'Exact' flux-weighted cross sections and conventional diffusion coefficients can be computed, since the flux distribution is assumed to be known. Assuming that the known heterogeneous surface currents are imposed on the two surfaces of node i, the diffusion problem is fully specified. This is a direct result of the fact that the diffusion equation is a second-order differential equation with known (and constant) coefficients—assuming k_{eff} is known. If one demands that the surface currents be preserved for both of these nodes, there will exist one, and only one, flux distribution which will satisfy the diffusion equation, as depicted in Fig. 3(b).

Since the homogenized flux distribution in each node is directly affected by the value of the diffusion coefficients, and the choice of flux weighted diffusion coefficients is in a sense entirely arbitrary, the interface fluxes will in all probability be different, as depicted in Fig. 3(c). This results from the fact that flux weighting of diffusion coefficients is only one of many possible methods for specifying the diffusion coefficients, and for *any* particular choice of diffusion coefficients, the homogenized surface fluxes will take on different values. As a direct result of the difference between interface fluxes, the homogenized flux distributions in both node i and node $i+1$ will be different than those of Fig. 3(c) when the two-node homogenized diffusion problem is solved with boundary conditions J_i^- and J_{i+1}^+, and continuity of flux and current interface conditions. An inevitable result of the different flux distributions in Fig. 3(d) is that the homogenized fluxes at the nodal interface will not be equal to the heterogeneous flux, and more importantly, the homogenized currents will not be equal to the heterogeneous interface current. From this example one can see that it is the interface condition, continuity of flux, and not the values of diffusion coefficients, which cause the

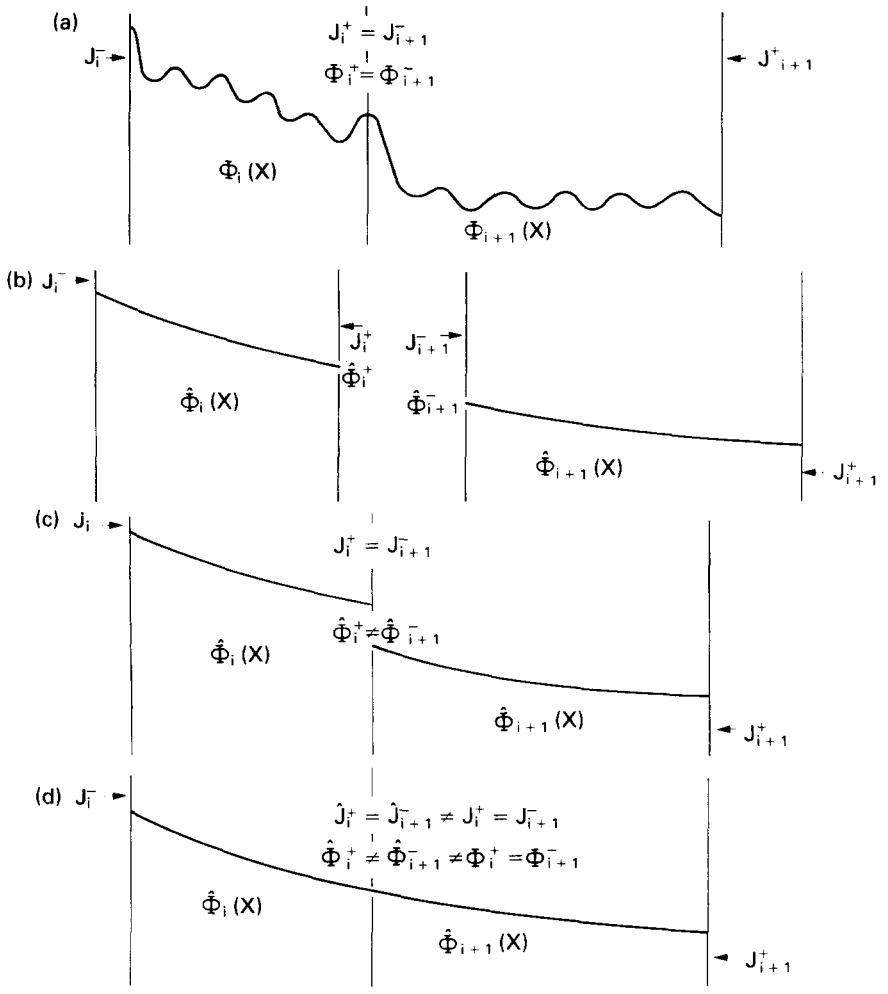

Fig. 3. One-dimensional nodal flux distributions.
(a) Heterogeneous reactor flux.
(b) Individual homogenized nodes.
(c) Adjacent individual homogenized nodes.
(d) Conventional diffusion solution to the two-node problem.

homogenized currents to be different from the reference currents. One could adjust D_i and D_{i+1} such that

$$\hat{\Phi}_i^+ = \hat{\Phi}_{i+1}^- = \Phi_i^+,$$

and imposing continuity of flux would no longer be a problem. However, one must also consider preservation of current between node i and node $i-1$ and in this case the freedom to adjust D_i would have already been used by preserving the current between node i and node $i+1$. It is clear, now, that the homogenized diffusion equation (with continuity of flux and current across interfaces) lacks sufficient degrees of freedom to allow simultaneous preservation of reaction rates and currents.

3.2. *Koebke's homogenization method*

Traditionally, advanced homogenization methods have been developed in order to improve the accuracy of node-averaged reactor properties predicted through use of conventional homogenized parameters. Koebke's homogenization method, Equivalence Theory,[26,45–47] which represents the most significant advance in homogenization methods to date, was motivated in large part by efforts to address the PWR dehomogenization problem[19,48] (i.e. predicting pin power distributions from nodal solutions). Koebke observed that there exists a very close connection between the homogenization and dehomogenization problems, and improvements in predicted

pin power distributions could be achieved only by a redefinition of the homogenized parameters.[48] Koebke not only recognized the difficulty in preservation of surface currents, but was able to formulate a mathematical interface condition which allowed exact preservation of both reaction rates and net currents from heterogeneous reactor problems. Koebke recognized the important point that if the homogenized fluxes are allowed to be discontinuous the homogenized flux distribution, such as that depicted in Fig. 3(c), could be preserved when the two-node homogenized boundary value problem is solved. Consider the flux distribution of Fig. 4. When the two-node boundary value problem is solved, the homogenized flux distributions will be identical to those of Fig. 4 if an interface condition is imposed such that

$$\hat{\Phi}_i^+ f_i^+ = \hat{\Phi}_{i+1}^- f_{i+1}^-, \tag{9}$$

where

$$f_i^+ \equiv \Phi_i^+ / \hat{\Phi}_i^+, f_{i+1}^- \equiv \Phi_{i+1}^- / \hat{\Phi}_{i+1}^-.$$

This equation expresses that the heterogeneous flux is continuous across the interface and that there exists a direct relationship between the heterogeneous and homogenized surface fluxes. When the homogenized two-node problem is solved, the homogenized flux is made discontinuous (by a factor of f_i^+/f_{i+1}^-) and the homogenized flux distribution will be the same as that in Fig. 3(c), which results in the preservation of interface currents. The equivalence factors (f_i^+ and f_{i+i}^-) can be considered to be additional homogenization parameters (as are cross sections and diffusion coefficients) since they can be defined directly from information which is known from the reference solution. These equivalence factors provide additional degrees of freedom which permit simultaneous preservation of reaction rates and surface currents.

The arguments of the preceding section rely on the uniqueness of the solution to the one-dimensional differential neutron diffusion equation with one energy group. The true utility of Koebke's homogenization method is that it is applicable to the case of many energy groups and multi-dimensional geometry. The mathematical formulation of the two-dimensional multigroup boundary value problem can be derived from the homogenized diffusion equation for node ij

$$-\nabla \cdot \hat{D}_{gi,j} \nabla \hat{\Phi}_g(x, y) + \hat{\Sigma}_{tgi,j} \hat{\Phi}_g(x, y) = \sum_{g'=1}^{G} [1/k_{\text{eff}} \hat{M}_{gg'i,j} + \hat{\Sigma}_{gg'i,j}] \hat{\Phi}_{g'}(x, y), \tag{10}$$

where the cross sections are flux-volume weighted, and both cross sections and diffusion coefficients are spatially constant within node ij. The conditions of equation (4) do not require that the homogenized surface currents match the heterogeneous surface currents, but only that the face-averaged currents be preserved. Therefore, the differential equations which the homogenized fluxes must obey can be determined by treating the directions one at a time and integrating over the directions transverse to those of interest in order to obtain for direction 'u' and node ij

$$-\hat{D}_{gi,j} \frac{d^2}{du^2} \hat{\Phi}_g(u) + \hat{\Sigma}_{tgi,j} \hat{\Phi}_g(u) - \sum_{g'=1}^{G} [1/k_{\text{eff}} \hat{M}_{gg'i,j} + \hat{\Sigma}_{gg'i,j}] \hat{\Phi}_g(u) = -\hat{S}_{gi,j}(u), \tag{11}$$

$g = 1, 2 \ldots G$
$u = x, y$
$v = x, y$ not $= u$

where

$$\hat{\Phi}_g(u) = \int_{v_i}^{v_{i+1}} dv \hat{\Phi}_g(u, v)$$

$$\hat{S}_{gi,j}(u) = \hat{D}_{gi,j} \int_{v_i}^{v_{i+1}} dv \frac{d^2}{dv^2} \hat{\Phi}_g(u, v).$$

By virtue of the fact that the heterogeneous reactor solution has been assumed to be known, the net

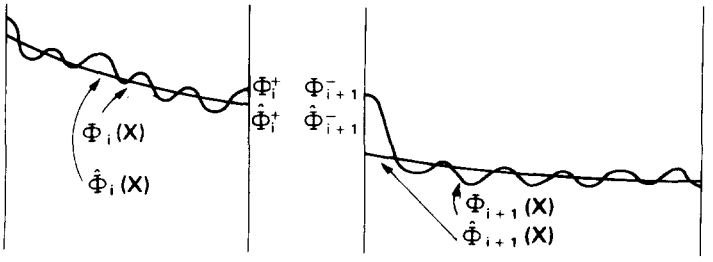

Fig. 4. One-dimensional nodal flux distributions.

leakage distributions, $\hat{S}_{gi,j}(u)$, is also known. Equation (11) and two appropriate boundary conditions per group constitute a well-posed one-dimensional boundary value problem for the one-dimensional homogenized flux distributions in node i, j. Therefore, with the net leakage distribution assumed to be known from the reference solution and with $J^{u+}_{gi,j}$ and $J^{u-}_{gi,j}$ as boundary conditions, equation (11) can be solved to obtain the one-dimensional flux distributions. Equivalence factors can then be defined from equation (9). The boundary value problem must, necessarily, be solved for all groups simultaneously since the shape of the homogenized flux in group g will affect the shape of the flux in group g' when there is scattering or fission transfer between groups.

The procedure for evaluating the equivalence factors appears to be straightforward. In two or more dimensions, however, the values of the equivalence factors will be correct (i.e. preserve interface currents) if and only if the net leakage distribution in the homogenized problem is the same as the net leakage distribution in the heterogeneous problem. The homogenized leakage distribution clearly cannot be expected to display the same fine structure as the heterogeneous leakage distribution. Consequently, the values of the equivalence factors will not preserve the true heterogeneous currents.

Fortunately, Koebke recognized that it is not as important to have the correct heterogeneous leakage distribution as it is to use the same leakage distribution, whatever it is, both when solving equation (11) for equivalence factors and when solving the global homogenized diffusion equation.

As yet there has been no discussion concerning which method for solving the diffusion theory boundary value problem and obtaining equivalence factors should be used. A subtle but very important point to realize is that *any approximate method* can be used and exact equivalence factors can be determined. These equivalence factors will preserve all interface currents when the global homogenized diffusion equation is solved, providing that the *identical* approximate method is used for solving the global diffusion equation. In fact, equation (11) can be solved with the one-mesh-point-per-assembly finite-difference approximation and exact homogenized parameters can be defined. This aspect of Koebke's 'Equivalence Theory'[45] is unique, in that one does not attempt to find homogenized parameters which will reproduce (in an integral sense) the heterogeneous reactor solution when the homogenized differential reactor equations are solved *exactly*, but rather, one defines homogenized parameters which reproduce the heterogeneous solution even though the homogenized reactor equations are themselves solved *approximately*. For example, many nodal methods[9] employ the transverse integrated diffusion equation, equation (11), as their basic nodal coupling relationship. In these methods the transverse leakage distribution is typically expanded as a quadratic polynomial such that the average values of the transverse leakages are preserved in three neighboring nodes. For these methods, it is straightforward to solve equation (11) since the average values of the transverse leakages are known from the heterogeneous solution. For methods such as fine-mesh finite-difference, it is difficult, if not impossible, to know what the transverse leakage shape will be when the homogenized diffusion equation is solved, and consistency between source terms is difficult to satisfy precisely.

Koebke's homogenization method makes further use of the fact that exact values of the equivalence factors can be found for any value of the diffusion coefficient. For an arbitrary value of the diffusion coefficients, the values of f^{u+} and f^{u-} for node i, j will be different. Koebke's method iterates on values of the diffusion coefficients for node i, j such that f^{u+} and f^{u-} are the same. When this condition is met, the resulting diffusion coefficients and *heterogeneity factors* (f^{u}_{g}) are considered as additional homogenization parameters which, in general, will be direction dependent. This homogenization method is known as 'Equivalence Theory' (E.T.), and when these parameters are employed, the homogenized diffusion equation can be solved such that k_{eff}, all surface-averaged currents, all node-averaged fluxes, and all node-averaged reaction rates are simultaneously preserved.

3.3. *General equivalence theory*

Koebke's homogenization method provides a well-defined, systematic method for determining homogenized parameters which will preserve the desired properties of the heterogeneous reactor solution when used in the homogenized diffusion equation. Koebke's method of constraining the diffusion coefficients such that heterogeneity factors are, for a given direction and group, identical on both surfaces of a node requires that an iterative method be used to determine diffusion coefficients. Although this iteration is numerically straightforward,[48] there exists a simple method for avoiding the iterative determination of the diffusion coefficients. This variation of Koebke's homogenization method[33,49] merely takes advantage of the fact that exact heterogeneity factors can be defined from equation (9) for any value of the diffusion coefficient. Note that unless the diffusion coefficients are found iteratively the values of the heterogeneity factors on

opposite faces of a node will be different. These two factors are referred to as *discontinuity factors* to distinguish them from heterogeneity factors, and they are defined by the following expressions,

$$f^{u-}_{gi,j} \equiv \frac{\Phi^u_{gi,j}(u_l)}{\hat{\Phi}^u_{gi,j}(u_l)}, \qquad f^{u+}_{gi,j} \equiv \frac{\Phi^u_{gi,j}(u_{l+1})}{\hat{\Phi}^u_{gi,j}(u_{l+1})}, \tag{12}$$

where u_l and u_{l+1} represent the lower and upper u-direction boundaries of node$_{i,j}$. Although exact reproduction of a reference solution is possible for any values of diffusion coefficients, Smith[49] chose to use the conventional flux-volume weighted diffusion coefficients. The reasons for this choice become clear when 'Generalized Equivalence Theory' (G.E.T.)[33,49] is applied to problems in which reference solutions are not known.

3.4. *Implementation of nodal equivalence theories*

Equivalence Theory, or Generalized Equivalence Theory, can be incorporated directly into any nodal method which uses nodal surface-averaged fluxes in the process of evaluating nodal coupling. Koebke[45] successfully modified the NEM code, demonstrating that heterogeneous reference solutions could be reproduced by using heterogeneity factors. Smith, likewise, modified the QUANDRY code and further demonstrated that even the coarse-mesh finite-difference (CMFD) method could reproduce heterogeneous reference solutions using discontinuity factors. The expression for nodal interface current on the upper u-direction surface of node i,j in the CMFD approximation can be written as

$$\hat{J}^u_{gi,j} = \frac{2D_{i,j}D_{i+1,j}}{h_i h_{i+1}} \cdot \frac{[f^{u+}_{gi,j}\hat{\Phi}_{gi,j} - f^{u-}_{i+1,j}\hat{\Phi}_{gi+1,j}]}{[f^{u-}_{gi+1,j}D_{gi,j}/h_i + f^{u+}_{gi,j}D_{gi+1,j}/h_{i+1}]}, \tag{13}$$

where $\hat{\Phi}_{gi,j}$ and $\hat{\Phi}_{gi+1,j}$ are the node averaged fluxes, and h_i and h_{i+1} are the mesh spacings in node i,j and node $i+1,j$, respectively. There are several things worth noting from this relationship. First, if discontinuity factors on opposite sides of an interface are the same, the discontinuity factors will have no influence on the interface current. This is true regardless of the nodal method to which discontinuity factors are applied. Secondly, although the form of equation (13) is similar to that of ordinary CMFD approximations, there is one important difference. Even when the diffusion coefficients and mesh spacings are the same in node i,j and node $i+1,j$, the form of equation (13),

$$\hat{J}^u_{gi,j} = \frac{2D[f^{u+}_{gi,j}\hat{\Phi}_{gi,j} - f^{u-}_{i+1,j}\hat{\Phi}_{gi+1,j}]}{h[f^{u-}_{gi+1,j} + f^{u+}_{gi,j}]}, \tag{14}$$

is not the same as that of the CMFD current,

$$\hat{J}^u_{gi,j} = \frac{2D}{h} \cdot [\hat{\Phi}_{gi,j} - \hat{\Phi}_{gi+1,j}]. \tag{15}$$

The significant difference between equations (14) and (15) is that equation (14) cannot be written in the form

$$\hat{J}^u_{gi,j} = C_{i,j} \cdot [\hat{\Phi}_{gi,j} - \hat{\Phi}_{gi+1,j}]. \tag{16}$$

This is significant in that most finite-difference diffusion codes utilize and store the symmetric operator $C_{i,j}$, whereas the current equation with discontinuity factors requires storage of two coefficients per interface. Nonetheless, implementation of heterogeneity factors or discontinuity factors into existing nodal codes is straightforward.

3.5. *Difference between equivalence and generalized equivalence theory*

The only assumption required in order to evaluate homogenization parameters for either form of equivalence theory is that the heterogeneous reactor solution be known. The goal of spatial homogenization, however, is to be able to predict accurately the solution to the heterogeneous reactor without actually solving the heterogeneous problem. Therefore, any homogenization method is of little practical value if it requires that the heterogeneous reactor solution be known in order to define homogenized parameters.

One straightforward means of demonstrating the differences between Equivalence Theory and Generalized Equivalence Theory is to examine a simple homogenization problem. Consider the one-dimensional 2-group problem, depicted in Fig. 5, in which a PWR-like fuel assembly which has all of its burnable poison pins in one half is positioned between an unpoisoned and fully poisoned assembly. This situation is similar to first-cycle cores in which burnable poison is preferentially loaded toward the core center side of some peripheral assemblies. The cross sections for type 'A' and 'B' assemblies were chosen to be identical except for the thermal absorption which is 12% higher in the type B assembly. Zero net current boundary conditions are assumed on all outer boun-

	A	A	B	B
Relative Assembly Powers	1.371	0.9823		0.6460

Fig. 5. A one-dimensional homogenization problem.

Table 3. E.T. and G.E.T. parameters for the AB assembly

Quantity	E.T. parameters	G.E.T. parameters
Σ_{a2}, (cm^{-1})	0.084219	0.084219
f_1^-, f_1^+	0.999	$f_1^- = 1.036, f_1^+ = 0.9508$
f_2^-, f_2^+	0.998	$f_2^- = 1.0856, f_2^+ = 0.8919$
D_1, (cm)	1.101	1.320
D_2, (cm)	0.088	0.383

daries. A full description of this problem is given in Appendix 1.1. A QUANTM diffusion theory reference solution to this problem was computed and used to generate E.T. and G.E.T. parameters for the central assembly (see Table 3).

Since assemblies A and B are homogeneous, and since QUANTM has no spatial truncation error in one-dimensional problems, the A and B assembly discontinuity factors and heterogeneity factors are unity. Both sets of parameters reproduce the reference solution exactly. Since conventional diffusion theory overpredicts the leakage from assembly A to assembly B, equivalence theory diffusion coefficients are necessarily reduced in order to match the reference solution. Because of the fact that the discontinuity factors are almost antisymmetric from one side of the AB assembly to the other, the heterogeneity factors are almost unity. The reference discontinuity factors (RDFs) reproduce the reference solution, but in a very different manner than do the reference heterogeneity factors (RHFs) and equivalence theory diffusion coefficients. The conventional solution to this problem, using unity discontinuity factors (UDF) and reference flux weighted cross sections (RXS), is compared to the reference in Table 4.

The important question, however, is 'How well do the equivalence parameters work when the AB assembly is surrounded by assemblies which are different from those used in the reference configuration?', that is, when a reference solution is not used to compute equivalence parameters. As a test of the applicability of the reference equivalence parameters, assembly B was replaced by assembly type C (a homogeneous assembly which had the average thermal absorption cross section of types A and B). The solutions to this problem obtained with reference discontinuity factors, reference heterogeneity factors, and unity discontinuity factors (as defined from the original problem), are compared to the reference solution in Table 5. As in the previous problem, conventional diffusion theory over predicts the leakage through the AB assembly. The RHFs correct about one half of the diffusion theory error and RDFs correct almost all of the diffusion theory error.

The differences between equivalence and generalized equivalence parameters can be graphically demonstrated when assembly B of Fig. 5 is replaced by assembly A, that is, a situation in which an AB assembly is positioned between two type A assemblies. The results for this problem are given in Table 6.

These results demonstrate that the discontinuity factors accurately predict the power distribution on this problem, despite the fact that the power distribution here is very different from the one for which they were generated. The use of heterogeneity factors yields almost the same solution as diffusion theory, because the heterogeneity factors are approximately unity. The significance of this problem is that both diffusion theory and Equivalence Theory view the homogenized problem as being symmetric about the central assembly—which it is not. In fact, this problem demonstrates one case in which heterogeneity factors cannot reproduce a reference solution, even when the solution is known.

An analogous situation can be envisioned in which the use of discontinuity factors might encounter

Table 4. Comparison of solutions to the one-dimensional homogenization problem

	k_{eff}	Assembly A power	Assembly AB power	Assembly B power
Reference solution	1.04514	1.371	0.983	0.646
Error in RXS-UDF solution	−0.12%	−3.1%	+0.3%	+5.9%
Error in RXS-RDF solution				
RXS-RHF solution	0.0%	0.0%	0.0%	0.0%

Table 5. Approximate solutions to the 1-dimensional homogenization problem

	k_{eff}	Assembly A power	Assembly AB power	Assembly C power
Reference solution	1.05287	1.248	0.967	0.786
Error in RXS-RDF solution	+0.05%	−0.2%	+0.5%	−0.3%
Error in RXS-RHF solution	+0.02%	−1.6%	+0.1%	+2.4%
Error in RXS-UDF solution	−0.02%	−3.9%	+0.4%	+5.7%

Table 6. Approximate solutions to the modified 1-dimensional problem

	k_{eff}	Assembly A power (error)	Assembly AB power (error)	Assembly A power (error)
Reference solution	1.06564	1.080 (ref.)	0.940 (ref.)	0.980 (ref.)
RXS-RDF solution	1.06688	1.078 (−0.3%)	0.950 (+1.1%)	0.972 (−0.8%)
RXS-RHF solution	1.06704	1.030 (−4.7%)	0.940 (0.0%)	1.030 (+5.1%)
RXS-UDF solution	1.06696	1.027 (−4.9%)	0.946 (+0.6%)	1.027 (+4.9%)

difficulties in modeling a symmetric situation. Consider the situation in which the AB assembly in the original one-dimensional problem is constructed with fuel type B (10.5 cm thick) positioned between two segments (5.25 cm thick) of type A fuel. In this homogenization problem, the central assembly which is symmetric, is located in an asymmetric environment. When reference discontinuity factors are generated for this situation and then used in the problem in which the central assembly is positioned between two type A assemblies, the resulting power distribution will be asymmetric. Heterogeneity factors, on the other hand, will reproduce this symmetry even though they were generated in an asymmetric situation. The results of QUANTM calculations for this symmetric situation are displayed in Table 7. The magnitude of the asymmetry in the discontinuity factor solution is approximately 0.3%. This asymmetry is quite small because the reference discontinuity factors are nearly symmetric, despite the fact that they were generated in a very asymmetric environment.

These calculations demonstrate one of the basic differences between heterogeneity factors and discontinuity factors: heterogeneity factors guarantee a symmetric response matrix, while discontinuity factors do not.[48] In the case of symmetric assemblies, there is very little difference (in accuracy) between the two approaches. Although the case of asymmetric assemblies may seem contrived, this combination of assemblies does occur in many first cycle PWR cores. In such cases, caution should be exercised in the use of heterogeneity factors, although difficulties can easily be avoided by using reactor representations in which assemblies are homogenized by quadrants and four nodes per assembly are used in the nodal calculations.

Although the one-dimensional homogenization problem may not be a very meaningful test of homogenization methods, the HAFAS BWR problem is. The reference solution to the HAFAS problem was used to generate reference discontinuity factors (RDFs) and reference cross sections (RXSs). The actual values of RDFs are different in every node, however,

Table 7. Approximate solutions to the symmetric 1-dimensional problem

	k_{eff}	Assembly A power (error)	Assembly ABA power (error)	Assembly A power (error)
Reference solution	1.06551	1.036 (ref.)	0.929 (ref.)	1.036 (ref.)
RXS-RDF solution	1.06537	1.039 (+0.3%)	0.928 (−0.1%)	1.033 (−0.3%)
RXS-RHF solution	1.06537	1.036 (0.0%)	0.928 (−0.1%)	1.036 (0.0%)
RXS-UDF solution	1.06519	1.031 (−0.4%)	0.938 (+1.0%)	1.031 (−0.4%)

certain patterns emerge when the discontinuity factors are examined as a function of assembly type. Some of the RDFs for the HAFAS BWR benchmark problem are displayed in Table 8. It can be seen from these results that the thermal discontinuity factors range from approximately 0.65 to approximately 1.70. Discontinuity factors for a particular assembly type also are quite different depending on the surface type (i.e. narrow or wide water gap). For a given assembly type and surface type, however, the RDFs display little variation. Realizing that RDFs are quite insensitive to the location of the assembly within the reactor, Smith [33,49] proposed a simple method for determining accurate, though approximate, discontinuity factors which do not require knowledge of full heterogenous solutions.

3.6. *Evaluations of discontinuity factors from assembly calculations*

If equivalence parameters were strictly a function of assembly type and did not depend on assembly boundary conditions, they could be determined from heterogeneous assembly calculations.[33,49] When two-dimensional assembly calculations are performed for a given type of assembly, the resulting equivalence theory cross sections and diffusion coefficients are identical to flux-weighted constants (AXSs). Generalized Equivalence Theory also requires that values of the discontinuity factors be determined. It appears that an assembly calculation may not provide sufficient information to determine discontinuity factors. There exists, however, a homogeneous analog to the heterogeneous assembly calculation—a single-node problem with zero net current boundary conditions. In the analogous problem, the homogenized fluxes are spatially flat. Since the assembly-averaged fluxes in the homogeneous and heterogeneous assembly calculations are, by definition, equal, the discontinuity factors are simply ratios of the *surfaced-averaged fluxes* to the *cell-averaged fluxes* in the heterogeneous assembly calculation. It is, thus, possible to approximate all of the equivalence parameters by performing assembly calculations for each type of assembly. Such equivalence parameters are referred to as assembly discontinuity factors (ADFs). Although in this particular case the discontinuity factors are approximated by the ratio of surface to average flux in the heterogeneous assembly calculation, the ratio of surface-to-average flux does *not* define the discontinuity factor in general. In fact, the discontinuity factors will be very poorly approximated by the surface-to-average flux ratio in situations in which there is leakage across nodal interfaces (as in a multi-assembly lattice calculations). The ADFs for the HAFAS BWR problem are compared to mean values of the RDFs in Table 9.

Several conclusions can be drawn from the results of Table 9: (i) the ADFs are within a few percent of the mean values of the RDFs for all assembly types, surfaces, and groups, (ii) the fast group discontinuity factors are much closer to unity than are the thermal group discontinuity factors, and (iii) the wide gap discontinuity factors are much different than the narrow gap discontinuity factors.

The good agreement between ADFs and RDFs is encouraging in that the discontinuity factors for a particular type of assembly are quite insensitive to the assembly position in the reactor, and ADFs can be

Table 8. RDFs for the HAFAS problem

Node	Type of assembly	Thermal discontinuity factors	
		Wide gap	Narrow gap
(7, 1)	Unrodded A	1.465, 1.424	1.280, 1.271
(4, 2)	Unrodded A	1.466, 1.492	1.307, 1.271
(8, 2)	Unrodded A	1.486, 1.466	1.283, 1.288
(4, 3)	Unrodded A	1.431, 1.450	1.278, 1.249
(6, 4)	Unrodded A	1.472, 1.470	1.279, 1.275
(8, 4)	Unrodded A	1.476, 1.483	1.259, 1.244
(7, 5)	Unrodded A	1.481, 1.479	1.250, 1.266
(8, 6)	Unrodded A	1.481, 1.490	1.295, 1.285
(1, 1)	70% Void A	1.639, 1.639	1.301, 1.301
(3, 1)	70% Void A	1.613, 1.598	1.268, 1.298
(5, 1)	Rodded A	0.681, 0.630	1.684, 1.682
(6, 2)	Rodded A	0.645, 0.686	1.644, 1.648
(7, 3)	Rodded A	0.685, 0.626	1.671, 1.659
(4, 4)	Rodded A	0.660, 0.660	1.638, 1.638
(5, 5)	Rodded A	0.654, 0.654	1.655, 1.655

Table 9. Comparison of ADFs and RDFs from the HAFAS BWR problem

Assembly type	Surface type	Group 1		Group 2	
		ADF	Mean RDF	ADF	Mean RDF
Unrodded A	Wide gap	0.896	0.885	1.497	1.470
	Narrow gap	0.945	0.930	1.271	1.287
Rodded A	Wide gap	0.774	0.795	0.626	0.658
	Narrow gap	1.034	1.010	1.750	1.657
70% void A	Wide gap	0.908	0.902	1.641	1.622
	Narrow gap	0.954	0.946	1.300	1.292

computed directly from the information available in standard assembly calculations. As an example, an assembly calculation with zero net current boundary conditions was performed for the asymmetric AB assembly in the 1-dimensional homogenization problem presented in the previous section, and discontinuity factors were obtained ($f_1^- = 1.043$, $f_1^+ = 0.956$, $f_2^- = 1.098$, $f_2^+ = 0.901$). These discontinuity factors are quite close to the reference values displayed in Table 3. In addition, when ADFs and AXSs are used in the calculations of the three configurations of the asymmetric homogenization problem, the maximum errors in assembly powers are -1.1% (configuration A|AB|B), -0.5% (configuration A|AB|C), and -0.1% (configuration A|AB|A), respectively. The corresponding errors with conventional continuity conditions and flux weighted diffusion coefficients are 5.9%, 5.8%, and 5.1%. The fact that use of ADFs leads to accurate predictions of assembly powers in all three configurations implies that the true values of the discontinuity factors are well predicted by the single-assembly calculation. The fact that ADFs can be computed accurately from a conventional assembly homogenization calculation points out one difference between discontinuity factors and heterogeneity factors; in order to compute heterogeneity factors for asymmetric assemblies, it is necessary that there be leakage across assembly interfaces. Calculations of heterogeneity factors at KWU, in such special cases, have employed multi-assembly geometries in such a way that the diffusion coefficient iteration is possible.

Even though the good agreement between ADFs and RDFs is encouraging, the true test of any homogenization method is whether the solution to the heterogeneous reactor problem can be predicted accurately. The results of a QUANTM diffusion theory calculation of the HAFAS problem which used AXSs, ADFs, and assembly-sized mesh, are compared to the reference and conventional UDF solutions in Table 10. A complete comparison of the octant power maps is presented in Fig. 6. The use of ADFs reduced the homogenization error by at least a factor of three when compared with the error in conventional AXS. The improvement is universal in that all assembly types are predicted much more accurately. This dramatic improvement in power distribution is typical of BWR applications of assembly discontinuity factors.

Table 10. Comparison of results to the HAFAS BWR using UDFs and ADFs

	UDFs	ADFs
Error in k_{eff}	-0.44%	-0.08%
Maximum error in assembly power	$+12.8\%$	$+3.9\%$
Average error in assembly power	$+5.5\%$	$+0.9\%$

4. APPLICATIONS OF E.T. AND G.E.T.

4.1. *PWR Applications*

The use of ADFs for BWR applications is prompted by the high degree of asymmetry which is present in BWR assemblies, particularly when control rods are inserted. PWRs, on the other hand, tend to have symmetric assemblies even when control rods are inserted. For this reason, heterogeneity factors are widely utilized for PWR analyses at KWU. In fact, a simplified version of Equivalence Theory called Simplified Equivalence Theory (S.E.T.)[46] has been adopted at KWU. In this approximation, the directional dependence of the diffusion coefficient and heterogeneity factors are suppressed in favor of using one diffusion coefficient and one heterogeneity factor per group. When only one heterogeneity factor per group is employed, it is possible to divide all cross sections and diffusion coefficients by the group heterogeneity factors, obtaining equations that can be solved using diffusion codes which have conventional continuity conditions on interface fluxes. This significantly reduces the number of homogenization parameters (i.e. the same as conventional homogenization meth-

Reference Heterogeneous *P*3 Solution Error in *P*1 AXS-UDF Solution Error in *P*1 AXS-ADF Solution					1.095 7.0% -0.3%	0.690 8.3% 0.0%	0.399 12.8% -0.9%
				1.478 3.0% -0.5%	1.204 4.0% 0.4%	0.996 5.8% -1.1%	0.513 7.7% -0.3%
			0.995 10.9% -2.2%	1.277 -1.0% 1.0%	1.370 3.5% -0.1%	0.978 3.3% -0.1%	0.641 8.0% -0.7%
		1.122 4.4% -3.9%	0.888 6.7% -1.0%	1.268 -4.0% -0.3%	1.100 -1.0% 1.2%	1.018 2.2% -1.1%	0.572 5.3% 0.2%
	1.591 -5.3% -0.3%	1.502 -7.6% 1.4%	1.382 -7.6% 0.8%	0.811 4.0% -3.5%	0.764 11.7% -1.7%	0.798 -1.7% -0.0%	0.590 4.8% -0.6%
1.609 -4.1% 0.1%	1.432 -6.2% 0.9%	1.675 -6.7% 1.9%	1.238 -8.7% 2.1%	0.857 5.1% -3.3%	0.650 9.9% 0.1%	0.839 -1.8% -0.5%	0.512 2.4% 0.3%
1.371 -3.9% 1.1%	1.197 -4.8% 2.2%	1.265 -6.9% -0.3%	1.051 3.1% -0.2%	0.943 7.1% -0.2%	1.024 -7.9% 1.5%	1.050 -4.0% 0.6%	0.807 -2.5% -0.1%	0.569 2.6% -0.6%

Fig. 6. ADF and UDF power distributions for the HAFAS BWR problem.

ods), simplifies data handling, and allows flux discontinuities to be accommodated directly into the cross sections.

One of the steps in Koebke's application of simplified equivalence theory involved comparing an explicit 4-group, 'pin-by-pin' model of a small PWR[46] to a 2-group homogenized nodal calculation. The MEDIUM-2 reference solution is the equivalent of a PDQ-type calculation with explicit baffle and reflector. Koebke utilized a two-assembly/baffle/reflector problem for the heterogeneous multi-assembly calculation from which approximate equivalence parameters (AHFs) were derived. The reference reactor and multi-assembly geometry are described in reference 46. The reference and S.E.T. power distributions are compared in Fig. 7. The simplified equivalence theory solution

Reference Heterogeneous Solution Error in S.E.T. Solution Error in S.E.T. Without Fuel AHFs Error in UDF Solution Error in UDF with Reflector AHFs			0.656 0.0% 0.1% 20.4% 1.1%	
		1.108 0.4% 0.3% -3.7% -0.1%	1.015 0.7% 0.9% 2.0% 0.8%	0.545 -0.2% 0.0% 22.5% 1.3%
	1.438 -0.1% -0.1% -8.3% 0.7%	1.274 -0.1% -0.1% -6.4% -0.6%	0.984 0.2% 0.2% -2.3% 0.0%	0.712 -0.4% -0.3% 11.6% 0.9%
1.550 -0.1% -0.2% -9.4% -0.9%	1.493 -0.1% -0.2% -8.9% -0.9%	1.322 -0.2% -0.2% -7.2% -0.7%	1.033 -0.1% -0.0% -3.4% -0.1%	0.755 -1.3% -1.2% 10.6% -0.2%

Fig. 7. Assembly power distributions for the KOEBKE PWR problem.

displayed is a QUANTM solution which employed Koebke's published equivalence parameters (Koebke's S.E.T. power distribution was not published). It can be seen from the results of Fig. 7 that the maximum error in assembly power for the S.E.T. solution is only 1.3%. Koebke's conventional diffusion solution, using UDFs, displayed a maximum error in assembly power of 17.2%. It is clear that the use of equivalence theory has greatly improved the accuracy of the homogenized solution. The ratio of heterogeneity factors in the type 'A' assembly to those of the type 'B' assembly are 1.0019/1.0051 and 0.9639/0.9658 for groups 1 and 2, respectively. Since the ratios of heterogeneity factors are almost unity, the homogenized solution should be insensitive to the heterogeneity factors in the core region. A homogenized solution to the Koebke PWR problem in which the fuel assembly heterogeneity factors were set to unity is compared to the reference solution in Fig. 7. It can be seen that the solution changes only a few tenths of a percent from the complete S.E.T. solution. Thus, it appears that in the unrodded reactor configuration the major improvement over conventional diffusion theory is due to the heterogeneity factor at the core/baffle interface.

In order to test this hypothesis, a conventional homogenized diffusion solution has been computed and is also compared to the reference solution in Fig. 7. This diffusion solution is the result of a QUANTM calculation in which the flux-weighted diffusion coefficients were used. The 2-group diffusion coefficients were derived from Koebke's collapsed equivalence parameters and are compared to Koebke's diffusion coefficients[46] in Table 11.

Koebke collapsed 2-group diffusion coefficients by flux weighting $1/D$. These diffusion coefficients are quite different from the S.E.T. diffusion coefficients which are computed directly from the multi-assembly calculation. A much better approximation is obtained by flux weighting the diffusion coefficients, which yields diffusion coefficients within 5% of the S.E.T. diffusion coefficients.

A QUANTM homogenized reactor solution which employed flux-weighted diffusion coefficients (AXS-UDF) is compared to the reference solution in Fig. 7. This solution has 20.0% error in assembly power. When these conventional diffusion coefficients and cross sections are used with the homogenized baffle/reflector heterogeneity factors (computed directly from the 3-assembly homogenization problem using flux weighted diffusion coefficients) the solution to the homogenized reactor problem has a maximum error of 1.3% in assembly power, as shown in Fig. 7. It can be concluded that, for this problem, conventional cross sections and diffusion coefficients are adequate to compute accurate power distributions, providing heterogeneity factors are computed for the homogenized baffle/reflector nodes.

The fact that an accurate power distribution may be computed without using heterogeneity factors for the fuel assemblies of the Koebke PWR problem does not imply that the heterogeneity factors do not serve an important role in reactor analysis. In the 'rods in' version of Koebke's PWR problem, the maximum error in assembly powers goes up to 4.0% when conventional diffusion coefficients, cross sections, and unity heterogeneity factors are used in the fuel. This reflects the fact that the ratios of heterogeneity factors between rodded and unrodded assemblies are 1.0097/1.0019 and 1.1187/0.9639 for groups one and two, respectively. The thermal group discontinuity factors are much greater than unity when control rods are inserted, and consequently, heterogeneity factors will improve the power distributions computed using homogenized nodal models. A similar situation exists when large numbers of burnable absorber pins are present in PWR assemblies, and heterogeneity factors successfully treat such situations. In addition, heterogeneity factors are quite useful in performing the heterogeneous flux reconstruction which is required to predict individual pin powers.[19,48] Koebke has also found that heterogeneity factors are needed to successfully model group-collapse effects which are present in

Table 11. Diffusion coefficient comparison

Quantity	Approximation		
	S.E.T D	Flux-weighted D	Flux-weighted $1/D$
Type A, D_1	1.464	1.509	1.210
Type B, D_1	1.436	1.517	1.215
Reflector, D_1	1.264	1.193	1.076
Type A, D_2	0.342	0.342	0.342
Type B, D_2	0.383	0.342	0.342
Reflector, D_2	0.578	0.248	0.248

situations in which rodded assemblies are adjacent to unrodded assemblies.[48]

4.1.1. *PWR baffle/reflector homogenization.* The PWR baffle causes a great many difficulties for the reactor analyst. Historically, nodal models have used empirical albedos to replace both the baffle and reflector.[15,35] Determination of albedos involves a lengthy trial and error procedure in which albedos are adjusted such that the nodal power distribution matches that of some higher-order solution. When nodal models improved to the point where homogenized parameters for baffle/reflector nodes could be easily and accurately modeled, the difficulty became finding appropriate values of homogenized parameters for baffle/reflector nodes. Since the baffle is a strong absorber adjacent to the outer fuel assemblies, the use of flux-volume weighted cross sections distributes the absorption over the entire baffle/reflector region, radically mispredicting the local fluxes and absorption rates. This misprediction leads to error in power distributions as large as 10–15%.

The baffle itself is not difficult to treat with 'pin-by-pin' models, such as PDQ, providing appropriate baffle cross sections can be defined. The difficulty of obtaining baffle cross sections arises primarily from the nonasymptotic nature of the neutron spectrum in the vicinity of the baffle and from the magnitude of the transport effects in the baffle and reflector. For these reasons, an appealing approach to generating baffle and reflector cross sections is to use extended-assembly calculations which model one or more fuel assemblies, the baffle, and reflector. The use of an assembly homogenization code (e.g. CASMO,[5] DIT,[4] MULTI-MEDIUM,[7] etc.) to perform this calculation assures that the multigroup, nonasymptotic spectral, and transport effects are adequately treated. Such calculations have been performed, the usual practice being to collapse baffle cross sections into two groups and perhaps to use g-factors to assure that finite-difference diffusion calculations will 'reproduce' the transport results. This approach produces baffle and reflector cross sections which accurately predict the neutronic behavior of the baffle and reflector, providing an explicit 'pin-by-pin' reactor model is used.

If extended-assembly calculations are performed to treat the baffle, flux and current distributions and reaction rates can be used directly to define homogenized cross sections and heterogeneity (or discontinuity) factors which accurately model the baffle and reflector. The inherent advantage of the heterogeneity or discontinuity factors is that they are chosen in such a way that the *nodal* model will reproduce the net currents at the core/baffle interface and the net reaction rates in both the fuel assembly and the homogenized baffle/reflector without explicitly representing the baffle.

A two-dimensional model of the Zion-1 core[30] was used as a reference problem to test the ability of equivalence parameters to model the baffle and reflector. In this particular problem, fuel assemblies were treated as homogeneous (previous calculations indicated that the baffle/reflector equivalence parameters are unaffected by fuel assembly heterogeneities) and the baffle and reflector were modeled explicitly, as depicted in the problem description of Appendix 1.2. A QUANTM $P3$ transport solution to the ZION problem was generated using 4 nodes per assembly, plus explicit baffle divisions. Transport theory rather than diffusion theory is required to treat correctly the baffle/reflector, because diffusion theory mispredicts neutron absorption and transmission in the baffle, even when the baffle is modeled explicitly. These errors in diffusion theory models are of the order of 4–8% in peripheral bundle powers. The reference solution to the ZION problem was used to compute homogenized cross sections and discontinuity factors for every

Table 12. ZION baffle/reflector discontinuity factors and albedos

Node	Discontinuity factor		Albedo[a]	
	Group 1	Group 2	Group 1	Group 2
(9, 1)	1.200	0.199	7.26	8.88
(9, 2)	1.209	0.195	7.35	8.85
(9, 3)	1.198	0.199	7.31	8.79
(9, 4)	1.181	0.190	7.13	8.97
(8, 5) x-direction[b]	1.184	0.216	12.59	9.78
(8, 5) y-direction[b]	1.203	0.224	9.21	8.57
(8, 6) x-direction	1.201	0.182	7.35	9.40
(7, 7)[b]	1.190	0.230	10.37	8.94

[a] Albedo defined here as flux/current.
[b] Inside corners.

homogenized baffle/reflector node. They are summarized in Table 12, along with reference values of albedos. It can be seen that the discontinuity factors are quite independent of their actual location. The discontinuity factors at the jagged edges of the core/baffle interface (inside corners) do differ significantly from those at the flat edges. The variation is only about 2% in group 1 and about 10% in group 2. The reference values of the albedos show much larger variations—the inside corners being as much as 70% higher than the flat albedos in group 1, while the thermal albedos display only about 10% variation. These results indicate that the nodal diffusion model may be much less sensitive to the variation in discontinuity factors than to the variation in albedos.

QUANTM one-mesh-per-assembly diffusion calculations using discontinuity factors from the (9, 1) node are compared to the reference (explicit baffle/reflector) transport solution in Fig. 8. This calculation used collapsed cross sections from the (9, 1) node to represent all of the homogenized baffle/reflector nodes and, thus, did not attempt to represent the higher absorption cross sections of the inside corner nodes. The analogous QUANTM solution, employing the albedos from the (9, 1) node to replace all reflector nodes, is also displayed in Fig. 8. The QUANTM calculation, using one set of discontinuity factors for every baffle/reflector node, has a maximum error in assembly power of approximately 0.8%. The corresponding calculation, employing one set of albedos, has a maximum error of 12.4%. The large errors are due to the fact that the albedos are poorly approximated for the inside corners. A QUANTM calculation which used the average albedos for the inside corners (taken directly from the reference solution) and the (9, 1) node albedo for all other surfaces is also compared to the reference solution in Fig. 8. The maximum error has been reduced to about 3.2%. If the albedos were allowed to be different on each assembly surface, it would be possible to find an albedo set which could better predict the power distribution. However, matching the reference solution is only one of the objectives of a method for modeling the baffle/reflector. Another desirable objective is that the power distribution be accurately predicted even when the reactor is at some state other than the reference state for which the albedos were determined. As an attempt to model such a change, the fuel compositions of the highly enriched outer fuel assemblies and the low enriched internal assemblies were interchanged in the ZION problem. A QUANTM $P3$ solution to the reconfigured ZION problem (with explicit baffle representation) is compared to solutions obtained from QUANTM diffusion theory calculations which used

Reference heterogeneous $P3$ solution				0.683	0.336	
Error using one discontinuity factor				−0.8%	−0.1%	
Error using one albedo				−6.6%	−12.4%	
Error using flat or inside corner albedo				1.9%	2.9%	
	k_{eff} 1.27525	1.085	0.862	0.546		
	1.27519	−0.5%	−0.4%	−0.5%		
	1.27466	−1.5%	−3.2%	−7.9%		
	1.27523	0.5%	1.3%	3.2%		
	1.232	1.217	0.897	0.735	0.332	
	0.2%	−0.2%	0.2%	−0.4%	0.2%	
	1.3%	−0.1%	−1.1%	−2.8%	−10.9%	
	0.3%	0.2%	0.9%	−1.5%	−2.0%	
1.424	1.465	1.171	1.083	0.725	0.455	
0.3%	−0.1%	−0.3%	0.0%	0.2%	0.0%	
2.6%	−0.3%	1.2%	−0.2%	−1.4%	−3.3%	
0.2%	−0.1%	0.3%	−0.1%	−0.1%	−1.1%	
1.554	1.651	1.375	1.356	1.029	0.930	0.506
0.3%	−0.1%	0.4%	−0.1%	0.3%	−0.4%	−0.1%
3.2%	2.5%	2.5%	2.9%	0.9%	−1.0%	−2.5%
0.1%	−0.3%	0.2%	−0.3%	−0.1%	−1.3%	−2.3%
1.600	1.751	1.508	1.548	1.239	1.163	0.801	0.520
0.4%	−0.1%	0.1%	−0.1%	0.3%	0.0%	0.4%	0.8%
3.3%	2.8%	3.0%	2.1%	1.9%	0.7%	0.0%	−2.0%
0.1%	0.4%	0.0%	−0.3%	0.0	−0.6%	−0.6%	−2.4%

Fig. 8. Assembly power distribution comparison for the ZION PWR problem.

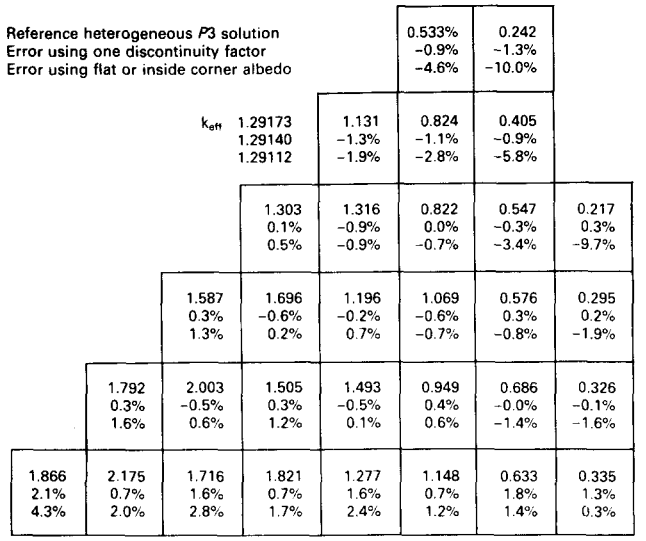

Fig. 9. Power distribution comparison for the modified ZION problem.

the initial configuration discontinuity factors and albedos in Fig. 9. It can be seen from these results that the maximum error in peripheral assembly power is only 1.9% for the discontinuity factor case, and the corresponding albedo case has a maximum error of 10.0%. This is significant in that the albedo set which produced only 3.2% error in the reference case has 10.0% error in the re-configured case. Thus, it is clear that the albedo values are attempting to model more than just the baffle and reflector, and that their values depend on the neutronics of the core regions which they adjoin. The nodal calculation which used the discontinuity factors does not display the large increase in error, and the discontinuity factors perform well in both the normal and re-configured cases.

It is important to remember that the use of albedos necessitates a two-dimensional reference solution in order to obtain normalization of the albedos. In contrast, one can utilize a single set of discontinuity factors and homogenized cross sections to represent the baffle/reflector nodes, and the resulting error will be small. Furthermore, these G.E.T. parameters can be taken from a one-dimensional calculation (as evidenced by the use of only the (9, 1) node parameters) or from a single extended-assembly calculation. Koebke has reported a more elaborate approach,[50] than the straightforward one reported here. In Koebke's approach, baffle/reflector diffusion coefficients and heterogeneity factors are adjusted to match the response matrices of the baffle/reflector as computed in two separate extended-assembly calculations. The extended-assembly calculations (in one-dimensional geometry) are performed for two different boundary conditions on the outer reflector surface. Koebke reports that the equivalence parameters are very insensitive to the boundary conditions. This implies that the equivalence parameters are applicable to a wide range of core conditions (e.g. power distributions, depletion, etc.). Homogenization of PWR baffle/reflector nodes represents one of the most significant applications of equivalence parameters in PWR analysis, and the necessity of performing fine-mesh two-dimensional quarter-core calculations to normalize albedos can be completely eliminated.

4.2. *Application of G.E.T. to a realistic 2-dimensional BWR configuration*

The results from the HAFAS BWR, KOEBKE PWR, and ZION PWR benchmark problems have demonstrated the significant improvement which results from the use of ADFs in homogenized reactor calculations. These results are sometimes discounted since all of these models involve significant compromises of the actual reactor configurations. In an effort to demonstrate that the conclusions from the benchmark problems translate directly to realistic reactor configurations, a much more realistic benchmark problem has been developed. The DVP BWR benchmark problem[51] models a fresh core at beginning of cycle. The two-dimensional model utilizes a control rod pattern and void distribution as computed by a three-dimensional reactor simulator, for a lower axial portion of core. This particular plane contains

40% voided assemblies except near the core periphery where assemblies are unvoided. Three control blades (in each quadrant) are modeled with 0% void conditions. The reference solution[51] to the DVP BWR problem is a two-group PDQ calculation which explicitly modeled all fuel pins, water gaps, control blades, and the reflector. Two-group pin-by-pin cross sections were obtained from full-assembly CASMO calculations, and g-factors were used so that single-assembly PDQ calculations matched the CASMO group-wise absorptions in control blades and burnable absorber pins. Homogenized cross sections and assembly discontinuity factors were computed from single-assembly PDQ calculations in order that the maximum degree of consistency was maintained between the reference solution and subsequent homogenized reactor calculations. The reactor description, homogenized cross sections and ADFs are given in Appendix 1.3. QUANTM solutions to the DVP BWR problem were generated using one-node-per-assembly mesh and the diffusion theory approximation.

The calculated power distributions computed with ADFs and UDFs are compared to the PDQ reference solution in Fig. 10 and summarized in Table 13. The conventional diffusion theory solution, using unity discontinuity factors, displays errors up to 13.5% in assembly power near the core periphery. In addition, powers in rodded assemblies are systematically overpredicted, by as much as 7.5%. The QUANTM calculation which used ADFs is in remarkably good agreement with the PDQ reference solution. The maximum error in assembly power is only 2.4%, and the powers in rodded assemblies are underpredicted, but by a small amount. The overall accuracy of the homogenized diffusion solution with ADFs is excellent, and errors are at least at factor of 3 less than the errors of the solution which used conventional continuity conditions. The DVP BWR problem clearly demonstrates that modern nodal methods in combination with ADFs are capable of predicting BWR power distribution with accuracies which approach that of explicit pin-by-pin models.

The fuel assemblies in the DVP BWR problem are all diagonally symmetric (a common fuel design). For such assemblies, there are only two unique discontinuity factors per group. However, these two discontinuity factors are quite different in magnitude since one is for the narrow gap and the other for the wide gap. Since only the ratio of discontinuity factors between assemblies is of consequence, it might be argued that the use of two discontinuity factors is not needed because, in the reactor, wide gaps always face wide gaps and narrow gaps always face narrow gaps. Thus the discontinuity factors at gap interfaces tend to cancel out. If this were true, one might use only the narrow gap discontinuity factors and divide all cross sections by these discontinuity factors, allowing conventional diffusion codes to be used to solve the homogenized problem. A QUANTM calculation for the DVP BWR problem which used only narrow gap discontinuity factors is compared to the other DVP BWR solutions in Fig. 10. One difficulty with this approach can be seen by examining the peripheral assembly powers. Bundles which have wide water gaps at the reflector interface have the incorrect discontinuity factors, and their powers are mispredicted by as much as 10%. This is not unexpected since the conventional UDF solution displays such errors, and the use of narrow gap discontinuity factors everywhere mistreats flux discontinuities at these interfaces.

Table 13. Results for the DVP BWR problem using UDFs and ADFs

Solution error	UDFs	ADFs
Error in k_{eff}	−0.16%	−0.03%
Maximum error in assembly power	13.5%	2.4%
Average error in rodded assembly power	5.5%	−1.5%

An additional difficulty with a one discontinuity factor approach occurs whenever the assemblies which surround a control rod have mismatched void conditions. The simple configuration depicted in Fig. 11. was calculated with homogenized cross sections and discontinuity factors from the DVP BWR problem. In this void-mismatch problem, the wide gap discontinuity factors do not cancel out, and the use of only narrow gap discontinuity factors predicts a solution (see Fig. 11) which has a flatter power distribution and errors up to 3% compared to the two discontinuity factor solution. The DVP BWR problem does not model depleted fuel assemblies, however, a similar mismatch in wide gap discontinuity factors occurs when there are exposure gradients as well.

ADFs are directly applicable in 3-dimensional geometry, although axial discontinuity factors should be unity since the axial void and exposure distributions are continuous within a given assembly. It should be recognized that Simplified Equivalence Theory has limitations when applied in 3-dimensional BWR geometry. Potential difficulties arise from the fact that cross sections have been divided by heterogeneity factors in order to introduce radial flux discontinuities. Consequently, axial void or exposure distributions will introduce axial flux discontinuities between nodes. This is a direct result of the fact that the discontinuity is necessary in the radial plane, while it is inappropriate

0.575 −1.0% −0.5% 5.3%	0.543 −1.5% −0.5% 6.9%	0.532 −1.3% −1.0% 7.0%		PDQ reference Solution Error in AXS-ADF QUANTM Solution Error in the Single ADF QUANTM Solution Error in the UDF QUANTM Solution						
0.896 −0.5% −0.6% 2.7%	1.042 −0.1% −0.4% 3.9%	0.909 0.2% 0.6% 5.1%	0.635 −0.4% 10.1% 13.5%	k_{eff} = 1.027008 k_{eff} = 1.026773 k_{eff} = 1.027014 k_{eff} = 1.025476						
1.196 0.1% −0.1% 1.9%	1.430 1.1% 1.0% 2.0%	1.318 1.4% 1.2% 1.9%	1.064 1.3% 1.2% 1.7%	0.761 −0.7% 0.8% 4.2%	0.583 −0.5% 1.3% 6.5%	0.510 1.7% 1.5% 5.0%				
1.362 0.2% −0.1% 1.0%	1.624 0.8% 0.6% 2.8%	1.534 0.8% 0.9% 3.2%	1.152 0.4% 1.1% 2.9%	0.964 −0.5% 0.3% 2.6%	0.830 −1.0% 0.2% 3.0%	0.807 0.1% 0.2% 3.6%	0.585 −1.4% 6.7% 10.5%			
1.356 0.0% −0.4% −0.7%	1.359 0.3% −0.0% −0.4%	1.317 0.3% 0.2% −0.0%	1.238 0.2% 0.2% 0.8%	1.155 0.3% 0.5% 1.6%	1.051 0.4% 0.6% 2.3%	0.929 0.3% 0.4% 2.2%	0.822 0.1% 0.5% 4.1%	0.508 1.4% 1.5% 8.2%		
1.248 0.0% −0.5% −3.0%	1.205 0.7% −0.3% −3.8%	1.203 0.4% 0.1% −3.6%	1.248 −0.2% −0.4% −1.7%	1.267 −0.2% −0.4% 0.4%	1.238 −0.2% −0.4% −0.3%	1.128 −0.4% −0.7% 0.5%	1.042 −0.6% −1.2% 1.8%	0.582 −1.6% 0.6% 5.4%		
1.092 0.7% 0.1% −6.3%	0.907 −1.8% −2.5% 6.6%	0.937 −2.4% −3.0% 6.9%	1.192 0.4% −0.0% −4.5%	1.327 0.2% −0.2% −1.5%	1.613 0.7% 0.4% 1.2%	1.501 0.7% 0.4% 1.8%	1.201 0.3% −0.7% 1.3%	0.726 −1.5% 0.2% 3.1%		
1.007 1.3% 0.5% −7.6%	0.821 0.1% −0.6% 5.8%	0.871 −1.3% −1.8% 5.0%	1.152 0.7% 0.1% −5.7%	1.311 0.3% −0.2% −2.5%	1.618 0.9% 0.5% 0.3%	1.506 0.7% 0.6% 1.4%	1.074 −0.8% 0.2% −1.0%	0.907 0.7% 0.6% 2.7%	0.530 −1.5% 9.4% 10.8%	
1.005 0.4% −0.5% −7.9%	0.971 1.2% −0.4% −8.2%	1.016 0.8% −0.0% −7.0%	1.136 0.0% −0.7% −5.3%	1.225 0.0% −0.6% −3.8%	1.252 0.0% −0.4% −2.8%	1.177 0.0% −0.2% −1.6%	1.024 −0.6% 0.7% −0.4%	0.852 −0.7% −0.5% −0.3%	0.701 1.0% −0.1% 2.2%	0.415 0.0% 0.4% 6.0%
0.973 0.5% −0.4% −8.8%	0.942 1.3% −0.4% −9.0%	0.979 1.0% −0.2% −8.2%	1.074 0.0% −0.7% −6.4%	1.116 −0.3% −1.0% −5.7%	1.075 0.3% −0.2% −5.7%	1.017 0.3% −0.1% −4.5%	0.959 −0.8% −1.0% −2.6%	0.858 −0.8% −1.1% −1.6%	0.780 1.1% 1.7% −0.1%	0.409 −2.4% 0.1% 3.8%
0.908 1.3% 0.3% −10.1%	0.749 −0.7% −1.6% 3.0%	0.783 −1.7% −2.8% 3.0%	0.990 0.7% −0.1% 8.4%	1.010 0.5% −0.2% −7.8%	0.823 −2.4% −3.0% −5.6%	0.771 −1.4% −1.8% −8.3%	0.886 −0.3% −0.7% −3.9%	0.848 −0.7% −1.1% −1.9%	0.802 −1.0% −1.8% −0.5%	0.431 −2.1% −0.7% 2.9%

Fig. 10. Power distributions for the DVP BWR benchmark problem.

Void Distribution Surrounding a Control Blade

0% void	40% void
40% void	0% void

Power Distribution

1.159 1.132	0.841 0.868
0.841 0.868	1.159 1.132

-Wide and Narrow Gap Discontinuity Factors
-Narrow Gap Discontinuity Factor

Fig. 11. Control rod void mismatch homogenization problem.

in the axial direction. This problem will be most pronounced when the axial mesh spacing is large, such that large burnup or void fraction differences occur between axial nodes.

5. FURTHER IMPROVED HOMOGENIZATION METHODS

5.1. *Introduction*

The case in favor of using ADFs for reactor analysis is easily made. It is of interest to know what causes the errors which remain when ADFs are used. It has already been demonstrated that node-averaged reaction rates are preserved exactly when reference cross sections (RXSs) and reference discontinuity factors (RDSs) are used. For this reason, the inaccuracies which do exist in the ADF solutions must be due to a combination of inaccuracies in homogenized cross sections and discontinuity factors. Some insight into the problem can be obtained from further examination of the HAFAS BWR problem, since reference equivalence parameters are known. In Fig. 12, the HAFAS reference and the QUANTM (AXS–ADF) solutions are compared to (a) a QUANTM calculation which used RXSs and ADFs and (b) a QUANTM calculation which used AXSs and RDFs. Comparisons between the RXS–ADF and AXS–ADF solutions show that using the reference cross sections rather than assembly cross sections actually leads to larger errors. One might expect that the RXS–ADF solution should be more accurate since the RXSs are the correct cross sections. Careful examination of Fig. 12 reveals that in virtually every assembly ADFs have led to a more accurate solution than either RXSs and ADFs or AXSs and RDFs. In fact, the use of RXSs (in place of AXSs) perturbs the solution in the opposite direction from using RDFs (in place of ADFs), and the magnitude of the changes are almost the same. The implication of these results is that errors in cross sections and discontinuity factors are in opposite directions and improving one or the other adversely affects the solution. This situation is not totally unexpected. AXSs and ADFs are a matched set of equivalence parameters, and their values are very much interrelated. The flux distribution which produces a set of cross sections also dictates the values of the surface

Reference Heterogeneous *P*3 Solution						1.095	0.690	0.399
Error in *P*1 AXS-ADF Solution						−0.3%	0.0%	−0.9%
Error in *P*1 RXS-ADF Solution						−3.9%	−3.3%	−7.6%
Error in *P*1 AXS-RDF Solution						3.8%	3.6%	7.4%
					k_{eff} 1.043129	1.478	1.204	0.996	0.513
					1.042251	−0.5%	0.4%	−1.1%	−0.3%
					1.043363	−2.1%	−1.4%	−3.3%	−4.4%
					1.042052	1.7%	1.9%	2.4%	4.4%
				0.995	1.277	1.370	0.978	0.641
				−2.2%	1.0%	−0.1%	−0.1	−0.7
				−2.0%	0.9%	−2.0%	−1.7	−5.3
				−0.3%	0.2%	2.0%	1.6	4.9
			1.122	0.888	1.268	1.100	1.018	0.572
			−3.9%	−1.0%	−0.3%	1.2%	−1.1%	0.2%
			−1.0%	0.4%	0.6%	0.4%	−3.0%	−3.5%
			−3.1%	−1.5%	−0.2%	0.7%	2.0%	3.9%
		1.591	1.502	1.382	0.811	0.764	0.798	0.590
		−0.3%	1.4%	0.8%	−3.5%	−1.7%	−0.0%	−0.6
		1.2%	4.5%	2.6%	−1.4%	−2.5%	−0.8%	−4.5
		−1.7%	−3.1%	−1.9%	−2.2%	0.8%	0.8%	4.2
	1.609	1.432	1.675	1.238	0.857	0.650	0.839	0.512
	0.1%	0.9%	1.9%	2.1%	−3.3%	0.1%	−0.5%	0.3%
	1.7%	2.9%	4.4%	4.4%	−1.8%	−0.6%	−1.9%	−3.0%
	−1.8%	−2.2%	−2.6%	−2.4%	−1.6%	0.6%	1.5%	3.5%
1.371	1.197	1.265	1.051	0.943	1.024	1.050	0.807	0.569
1.1%	2.2%	−0.3%	−0.2%	−0.2%	1.5%	0.6%	−0.1%	−0.6%
2.4%	3.8%	1.5%	1.3%	0.6%	2.9%	−0.1%	−1.0%	−4.4%
−1.5%	−1.8%	−2.0%	−3.6%	−1.0%	−1.5%	0.6%	0.9%	4.0%

Fig. 12. Power distribution comparison for the HAFAS BWR problem.

currents, and consequently, the discontinuity factors. Any direct effort to evaluate more accurate homogenized cross sections will have to be supplemented by an effort to improve estimates of discontinuity factors.

5.2. *Channel homogenization*

There is one indirect method of utilizing assembly calculations to further improve the accuracy of homogenized BWR nodal models. This method makes use of the hypothesis that much of the error in homogenized cross sections arises from inaccurate predictions of the relative fluxes between the fueled region of the homogenized assembly and the water gap (or rodded gap) regions of the assembly. To test this hypothesis, a nodal model can be constructed such that the fuel regions of the bundle and the water channel/control rod regions are treated separately. In this nodal model the ratio of fuel bundle to water channel/control rod fluxes can be different than in the assembly calculations.

This homogenization method is referred to, here, as 'channel homogenization'. The method utilizes identical assembly calculations which are to be used to get AXSs, but cross sections are collapsed over the regions shown in Fig. 13. Region '1' is the homogenized fuel bundle, and the regions numbered '2' are simply homogeneous water gaps. Regions '3' and '4' contain either homogeneous water (for unrodded assemblies) or homogenized control rods and water. In this 'nodal' reactor model a single channel region is used for the inter-assembly gaps, and the reactor model then has four nodes' per assembly—only one of which contains fuel. This nodal problem has an irregular mesh, but most modern nodal methods are quite capable of handling this situation.[9]

As a test of channel homogenization, the HAFAS assembly calculations were computed using the *P*3 transport option in QUANTM, and the corresponding channel homogenized cross sections (CHXSs) and discontinuity factors (CHDFs) were computed. An

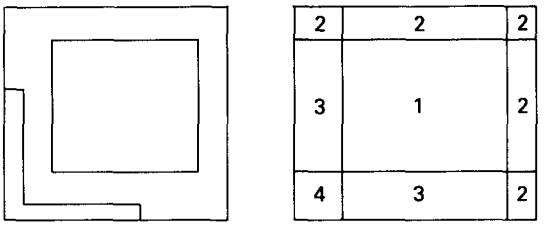

Fig. 13. Channel homogenization problem.

examination of the CHXSs and CHDFs reveals that the control blade/water cross sections are not influenced by the fuel type and only one set of equivalence parameters is required to model the control rods. The discontinuity factors for the control blade/water channel are very different from unity, 2.05 on the outer blade end and 0.47 on the blade center end, in the thermal group. This is to be expected since this region homogenizes a very strong neutron absorber with nonabsorbing water. A summary of several CHDFs is presented in Table 14. Water channel discontinuity factors (which arise, since the region is homogeneous, from spatial truncation and transport effects) are nearly unity and may be assumed to be independent of the assembly type or rodded configuration. Discontinuity factors for the fuel bundles are much closer to unity than in the ADF case and, as one might expect, much more like discontinuity factors for PWR bundles.

A QUANTM diffusion theory calculation with four nodes per assembly was performed using CHXSs and CHDFs. The resulting power distribution is compared to the reference solution in Fig. 14. It can be seen that the maximum error in assembly power is only 2.2%. The maximum error in rodded assembly power is reduced from 3.9% (ADFs) to only 1.8% in the CHXS-CHDF solution. Results of QUANTM calculations which used CHXSs and UDFs are also given in Fig. 14. The maximum error in assembly power is approximately 9.6%, demonstrating the importance of discontinuity factors in the channel representation.

Table 14. Channel homogenized discontinuity factors for the HAFAS BWR

Quantity	Assembly type			
	Unrodded A	Unrodded B	Rodded A	Unrodded B
Region 1 CHDFs[a]	1.063	1.059	1.022	1.015
Region 1 CHDFs[a]	1.068	1.063	1.114	1.109
Region 2 CHDFs[a]	0.986	0.984	0.986	0.989
Region 2 CHDFs[a]	1.039	1.036	1.078	1.083
Region 3 CHDFs[a]	1.022	1.025	0.491	0.473
Region 3 CHDFs[a]	1.031	1.030	2.045	2.063

[a] For group 2.

Reference Heterogeneous *P3* Solution					1.095	0.690	0.399
Error in *P1* AXS-ADF Solution					-0.3%	0.0%	-0.9%
Error in *P1* CHXS-CHDF Solution					-0.9%	-0.8%	-2.2%
Error in *P1* CHXS-UDF Solution					6.6%	7.8%	6.9%
			k_{eff} 1.043129	1.478	1.204	0.996	0.513
			1.042251	-0.5%	0.4%	-1.1%	-0.3%
			1.043363	-0.8%	-0.3%	-0.8%	-1.1%
			1.042735	3.3%	6.0%	6.4%	7.0%
			0.995	1.277	1.370	0.978	0.641
			-2.2%	1.0%	-0.1%	-0.1%	-0.7%
			-1.1%	0.3%	-0.3%	-0.5%	-1.4%
			3.7%	1.1%	3.6%	5.0%	5.0%
		1.122	0.888	1.268	1.100	1.018	0.572
		-3.9%	-1.0%	-0.3%	1.2%	-1.1%	0.2%
		-0.8%	-0.8%	0.1%	-0.2%	1.3%	-0.5%
		-4.5%	-5.7%	-3.5%	0.2%	1.4%	0.5%
	1.591	1.502	1.382	0.811	0.764	0.798	0.590
	-0.3%	1.4%	0.8%	-3.5%	-1.7%	-0.0%	-0.6%
	0.6%	1.6%	0.9%	-1.4%	-1.5%	-0.5%	-1.1%
	1.9%	-0.4%	-4.8%	-7.2%	-5.4%	-1.8%	0.3%
1.609	1.432	1.675	1.238	0.857	0.650	0.839	0.512
0.1%	0.9%	1.9%	2.1%	-3.3%	0.1%	-0.5%	0.3%
1.1%	1.4%	1.5%	1.5%	-1.8%	-1.1%	-1.0%	-0.9%
5.5%	3.7%	-0.2%	-4.6%	-9.6%	-7.9%	-4.9%	-1.4%
1.371	1.197	1.265	1.051	0.943	1.024	1.050	0.807	0.569
1.1%	2.2%	-0.3%	-0.2%	-0.2%	1.5%	0.6%	-0.1%	-0.6%
1.9%	1.9%	1.4%	0.5%	-0.2%	1.3%	0.0%	-1.1%	-2.0%
8.6%	7.6%	3.9%	-1.1%	-7.7%	7.3%	-6.6%	-4.6%	-3.6%

Fig. 14. Channel homogenized power distributions: HAFAS BWR problem.

The use of channel representation for BWRs is straightforward, and homogenization errors appears to be reduced to an acceptable level. The disadvantage in terms of computational effort (about a factor of four) may be unacceptable. One immediate advantage, however, is that the task of reconstructing pin-wise powers is much simpler in the channel representation. In fact, the BWR bundle in the channel representation appears much more like a PWR bundle. Also significant is the fact that parameterization of cross sections and discontinuity factors (versus exposure, void, etc.) is much simpler in the channel homogenized model.

5.3. *Extended-assembly homogenization*

Inaccuracies which result from the use of assembly homogenized parameters arise because the flux (and current) distributions which exist in the reactor assemblies are different from those obtained from single-assembly calculations. Interaction effects between assemblies are ignored when zero net current boundary conditions are imposed in the assembly calculation. If the actual boundary conditions which exist on the surface of an assembly were known, a fixed-source assembly calculation could be performed to obtain the correct homogenized parameters. Clearly, the required boundary conditions cannot be known unless the actual heterogeneous reactor solution is known. Nevertheless, the concept that accurate homogenization parameters can be obtained from assembly calculations using correct boundary conditions is a useful one.

The simplest means of obtaining more accurate estimates of boundary conditions is to use extended-assembly calculations.[22,25] Extended-assembly calculations typically include multiple assembly types (such as highly enriched and low enriched assemblies, rodded and unrodded assemblies, or peripheral assemblies and reflectors, etc.) and impose zero net current (or periodicity conditions) on the outer surfaces of the extended-assembly geometry. The resulting heterogeneous extended-assembly calculation will have non-zero currents between assemblies, and flux distributions will be different from those computed from single-assembly calculations. Extended-assembly calculations will produce more

accurate homogenized parameters, when the extended-assembly geometry is 'typical' of that encountered by the assemblies being modeled.

As an example of extended-assembly calculations in BWR, consider the rodded assemblies in the HAFAS BWR problem. Since each controlled bundle is surrounded by two uncontrolled bundles on the narrow gap sides, and two other controlled bundles on the wide gap sides, a natural extended-assembly calculation consists of one controlled bundle and three uncontrolled bundles with zero net current boundary conditions. A QUANTM $P3$ transport calculation was performed for both the type A and B rodded assemblies. Equivalence parameters derived from this calculation are compared to AXS–ADFs and to the mean RXS–RDFs of the reference heterogeneous solution in Table 15. It can be seen that results derived from the extended-assembly calculations are much closer to the mean values of the reference cross section and discontinuity factors than to the assembly cross sections and discontinuity factors.

Table 15. Comparison of extended-assembly homogenization parameters

Assembly parameter	Approximation ADF–AXS	Approximation Extended-assembly	Mean of reference
Type A, Σ_{a2}	0.05975	0.05826	0.05853
Type B, Σ_{a2}	0.05298	0.05209	0.05240
Type A, f_2^+	1.750	1.656	1.657
Type B, f_2^+	1.696	1.617	1.656
Type A, f_2^-	0.625	0.654	0.658
Type B, f_2^-	0.589	0.620	0.628

When the cross sections and discontinuity factors obtained from the extended-assembly calculation are used in the global homogenized model, it is found that the accuracy of the solution showed no improvement over the ADF–AXS solution. This is somewhat surprising since the homogenized parameters are closer to the mean values of the 'exact' homogenized parameters. Examination of the individual values of the RXSs and RDFs reveals that there is considerable scatter among the actual reference values. For instance, assembly type A thermal absorption cross sections range from 0.5808 to 0.5905, and type B wide gap thermal discontinuity factors range from 1.624 to 1.710. Thus, it would appear that the 'exact' equivalence parameters are sensitive to the actual details of the assembly flux distributions, and it is difficult to determine a 'typical' rodded environment in the HAFAS BWR problem.

The situation in PWRs is considerably more simple. The absence of control blades and the symmetries of PWR assemblies makes it much easier to utilize extended-assembly calculations. Koebke[46,47] has made extensive use of extended-assembly calculations for PWRs, with excellent results. Koebke has also reported that equivalence parameters can be represented as functions of the net assembly leakage rate. This allows cross sections to be recomputed (by examining individual assembly leakage rates) as the global homogenized diffusion equations are solved. In such a method, equivalence parameters are tailored, to some extent, to the local conditions of the flux distributions. This approach was examined for the HAFAS BWR problem, but was not successful. The asymmetric nature of the BWR bundles, particularly rodded bundles, seems to affect adversely the leakage rate parameterization. This can be seen by simply examining RDFs for the (4, 1) bundle in the HAFAS problem, in which the wide gap thermal discontinuity factors are 1.710 and 1.628. Despite the diagonal symmetry of the bundle, the RDFs are not symmetric. It appears that BWR assemblies are more sensitive to the local flux distributions than are PWR assemblies.

5.4. *Local fixed-source homogenization calculations*

One method of obtaining more accurate homogenized parameters is to utilize the 'rehomogenization' techniques discussed in Section 2.3.4. These methods use a solution to a global homogenized calculation (AXS–UDF or AXS–ADF) to obtain approximate reactor flux distributions which can be used to approximate boundary conditions for each assembly. When a fixed-source assembly (or extended-assembly) calculation is performed for each assembly, one obtains approximate equivalence parameters which reflect many of the inter-assembly effects. The resulting equivalence parameters can then be used to generate an improved global homogenized reactor solution, and presumably, the latter solution will be more accurate than its predecessor. The local fixed source calculation requires that some approximation be made for the spatial shapes of the surface sources. Spatial shapes from global homogenized reactor calculation cannot be expected to represent accurately the actual shapes of the sources on the surface of a heterogeneous assembly. The simplest shape, of course, would be to assume that the surface sources are spatially flat. Smith[33] demonstrated that the use of face-dependent, but spatially flat net current boundary conditions for the rehomogenization calculations lead to a reduction in maximum assembly error in the HAFAS problem (diffusion theory representation) from 5.3% to 2.1%.

Smith used a fine-mesh QUANDRY model to perform the local fixed-source calculations. Although this approach demonstrated that accurate homogenized parameters could be obtained by rehomogenization, the method is impractical as a tool for reactor analysis. The Combustion Engineering ROCS/MC[18] code allows cross sections to be rehomogenized (albeit with only cross sections and not discontinuity factors) during the global homogenized diffusion solution. The technique employed is to solve fine-mesh 2-group diffusion equations by imposing incoming partial currents which are taken from the nodal solution. The method works well for assemblies in the interior of the core but does not work well for peripheral assemblies. It has been found to require about $\frac{1}{7}$ of the time that would be required to solve the fine-mesh PDQ diffusion equations. In fact, if local heterogeneous calculation must be performed for every assembly, the nodal approach can be viewed as an acceleration technique for solving the global heterogeneous problem.

An alternative to performing local fixed-source calculations with explicit heterogeneous representation is to employ a response matrix formulation of the fixed-source problems. The advantage of this approach is that the difficult task of computing with heterogeneous detail need only be performed for each type of assembly (as functions of exposure, void, etc.). Subsequent fixed-source problems can then be performed with simple response matrix calculations. A large number of variations in the response matrix approach to rehomogenization have been developed at MIT.[20,25,52] These methods differ in the surface source (partial currents, net currents, or fluxes) and in the spatial shapes used in the response matrix calculations. The most successful of these approaches represents the surface flux as the product of quadratic polynomials and the heterogeneous flux shape obtained from a standard assembly calculation. This functional form accounts for much of the actual shape of the heterogeneous surface flux. Some convergence difficulties were encountered, and at least 3–4 iterations between global solution and response matrix calculations were required for convergence. This response matrix approach was shown to result in generalized equivalence parameters which reduce the error in assembly powers (for a very difficult BWR configuration in which a peripheral bundle was rodded) from 9.6% (using ADFs) to 1.1%.[20] These results clearly demonstrate that homogenization errors can be reduced to levels at which a great many other approximations become suspect. The drawbacks involved in using response matrix formulations are substantial. These include (i) the necessity of performing a great many response matrix calculations (the order of surface representation times number of surfaces times number of groups) for each state point in depletion, void, fuel temperature, etc., (ii) the large amount of data which must be handled during the global iteration (response matrices for each reaction rate, surface flux, surface current at each state point), and (iii) the necessity of recomputing the global diffusion solutions to obtain convergence. Response matrix methods have yet to be utilized in production codes, and the cumbersome nature of the response matrix data has deterred reactor analysts from adopting this approach.

6. OVERVIEW

The firm theoretical foundation for LWR assembly homogenization methods has been reviewed, and practical benchmark problems have illustrated that the use of flux-weighted cross sections and diffusion coefficients leads to large error (10–25%) in assembly power distributions. The primary source of error has been shown to arise from the treatment of homogenized flux continuity conditions at nodal interfaces. Koebke's Equivalence Theory and Smith's modification, Generalized Equivalence Theory, are capable of entirely eliminating homogenization errors, providing the global heterogeneous solution is known. Practical methods for obtaining approximate equivalence parameters were outlined, and these methods were successfully applied to PWR baffle/reflector homogenization and BWR bundle homogenization problems. Assembly discontinuity factors (ADFs), the simplest of the approximate equivalence methods, were shown to reduce BWR homogenization error by at least a factor of three relative to error in conventional homogenization methods. The ADF approach is attractive since discontinuity factors are derived from the very assembly calculations required by conventional homogenization methods. The use of extended-assembly calculations was successfully applied to the PWR baffle/reflector homogenization problem; it was demonstrated that a single set of cross sections and discontinuity factors can be used for all reflector nodes thus eliminating the conventional problem of determining surface-dependent albedos.

These homogenization techniques represent significant advances in homogenization theory, and their incorporation into nodal reactor models will result in considerable improvements in the predictive abilities of modern nodal methods. Information provided by advanced nodal models which utilize sophisticated homogenization methods can be combined with high-order pin power reconstruction (dehomogenization)

techniques to provide detailed power distributions. In fact, the goal of replacing detailed 'pin-by-pin' 2-dimensional models with 3-dimensional homogenized nodal models can be achieved without loss of accuracy.[26,47,48,49]

Residual homogenization errors were demonstrated to arise from inter-assembly interaction effects which cannot be predicted by single-assembly calculations. Sophisticated response matrix rehomogenization techniques have been demonstrated to be capable of reducing the homogenization errors well past the level of practical interest (1.0%). These techniques appear too cumbersome for practical applications, and further efforts should be directed towards establishing more efficient rehomogenization techniques.

LIST OF UNCONVENTIONAL ABBREVIATIONS

RXSs,	homogenized cross sections computed using reference reactor flux solutions.
AXSs,	homogenized cross sections computed using assembly flux solutions.
RHFs,	heterogeneity factors computed using reference reactor flux solutions.
RDFs,	discontinuity factors computed using reference reactor flux solutions.
ADFs,	discontinuity factors computed using assembly flux solutions.
UDFs,	Unity discontinuity factors (i.e. conventional continuity conditions).

Acknowledgements—The author would like to express his gratitude to a large number of individuals whose discussions have proved insightful and who have indirectly contributed to this document. These include R. D. Lawrence, A. F. Henry, E. M. Gelbard, D. M. Ver Planck, M. Edenius, C. Hoxie, and H. Khalil.

The author is also extremely grateful to K. Koebke for his efforts in reviewing this document and for his many helpful suggestions.

REFERENCES

1. Henry A. F. (1975) *Nuclear-Reactor Analysis*, The MIT Press, Cambridge, Massachusetts.
2. Gelbard E. M. (1981) Unfinished Monte Carlo business. *International Topical Meeting on Advances in Mathematical Methods for the Solution of Nuclear Engineering Problems*, Vol. 1, p. 145, Munich, 27–29 April.
3. Lewis E. E. and Miller F. W. (1984) *Computational Methods of Neutron Transport*, John Wiley and Sons, New York.
4. Jonsson A. and Grill S. F. (1978) Fuel assembly cross-section averaging for PWR fuel. *IAEA Technical Committee Meeting on Homogenization Methods in Reactor Physics*, Lugano, 13–15 November.
5. Ahlin A., *et al.* (1984) Integral transport computation of in-core gamma effects with CASMO/CPM. *Trans. Am. Nucl. Soc.* **47**, 434.
6. Ahlin A., *et al.* (1978) *CASMO User's Manual*, AE-RF-76-4518, Studsvik.
7. Wagner M. R. and Muller B. (1984) The nodal discrete ordinates method and its application to LWR lattice problems. *Topical Meeting on Reactor Physics and Shielding*, Vol. I, p. 376, Chicago, 17–19 September.
8. Halsall M. J. (1978) Some Practical Problems in LWR Box Homogenization. *IAEA Technical Committee Meeting on Homogenization Methods in Reactor Physics*, Lugano, 13–15 November.
9. Lawrence R. D. (1985) Progress in nodal methods for the solution of the neutron diffusion and transport equations, *Prog. Nucl. Energy*, this issue.
10. Walters W. F. and O'Dell R. D. (1980) Nodal methods for discrete-ordinates transport problems in $(x-y)$ geometry. *International Topical Meeting on Advances in Mathematical Methods for the Solution of Nuclear Engineering Problems*, Vol. 1, p. 115, Munich, 27–29 April.
11. Kavenoky A. (1978) The SPH homogenization method, IAEA-TECDOC 231, Lugano.
12. Cobb W. R. and Eich W. J. (1976) A new cell depletion code for LWR analysis. *Trans. Am. Nucl. Soc.* **24**, 442.
13. Yamamota M. (1982) Validation of the TGBLA BWR bundle design methods. *Trans. Am. Nucl. Soc.* **43**, 698.
14. Cadwell W. R. (1967) PDQ-7 reference manual, WAPD-TM-678, Bettis Atomic Power Laboratory.
15. Delp D. L., *et al.* (1964) FLARE, A three-dimensional boiling water reactor simulator, GEAP-4598, General Electric Company.
16. Gupta N. K., *et al.* (1981) Nodal methods for three-dimensional simulators. *Prog. Nucl. Energy* **7**, 127.
17. Nissen F. (1983) Determination of local pin powers in the framework of nodal coarse-mesh solutions. *A Topical Meeting on Advances in Reactor Computations*, Vol. I, p. 380, Salt Lake City, 28–30 March.
18. Jonsson A., Grill S. and Rec J. R. (1981) Nodal imbedded calculation for the retrieval of local power peaking from coarse mesh reactor analysis. *International Topical Meeting on Advances in Mathematical Methods for the Solution of Nuclear Engineering Problems*, Vol. 2, p. 23, Munich, 27–29 April.
19. Koebke K. and Wagner M. R. (1977) The determination of pin power distribution in a reactor core on the basis of nodal coarse mesh calculations. Atomkernenergi **30**, 136.
20. Finck P. J., Hoxie C. L., Khalil H. S., Parsons D. K. and Henry A. F. (1982) The application of nodal methods to light water reactors. *Proceedings of the Topical Meeting on Advances in Reactor Physics and Core Thermal Hydraulics*, Vol. 1, p. 348, Kiamesha Lake, 22–24 September.
21. Khalil H. S., Finck P. J. and Henry A. F. (1983) Reconstruction of fuel pin powers from nodal results. *A Topical Meeting on Advances in Reactor Computations*, Vol. I, p. 367, Salt Lake City, 28–30 March.
22. Hoxie C. L. (1982) Application of nodal equivalence theory to the neutronic analysis of PWRs. PhD Thesis, Department of Nuclear Engineering, M.I.T., Cambridge, MA, June.
23. Mendez-Castrillon J. F. P. (1984) Reconstruction of three-dimensional flux shapes from nodal solutions. MS Thesis, Department of Nuclear Engineering, M.I.T., Cambridge, MA, June.
24. Khalil H. S. (1983) The application of nodal methods to PWR analysis. PhD Thesis, Department of Nuclear Engineering, M.I.T., Cambridge, MA, January.
25. Cheng A. Y. C. (1981) Homogenization of BWR assemblies by response matrix methods. PhD Thesis, Department of Nuclear Engineering, M.I.T., Cambridge, MA, May.
26. Koebke K., Hetzelt L., Wagner M. R. and Winter H. J. (1984) Principles and application of advanced nodal

reactor analysis methods. *Topical Meeting on Reactor Physics and Shielding*, Vol. I, p. 134, Chicago, 17–19 September.
27. Wagner M. R., Koebke K. and Winter H.-J. (1981) A nonlinear extension of the nodal expansion method. *International Topical Meeting on Advances in Mathematical Methods for the Solution of Nuclear Engineering Problems*, Vol. 2, p. 43, Munich, 27–29 April.
28. Winter H.-J., Koebke K. and Wagner M. R. (1985) Solution of a two-dimensional PWR burnup benchmark problem by coarse mesh methods. *Proceedings of the International Meeting on Advances in Nuclear Engineering Computational Methods*, Vol. 1, p. 86, Knoxville, 9–11 April.
29. Smith K. S. (1986) Multidimensional nodal transport using the simplified P_L method. *Trans. Am. Nucl. Soc.* **52,** 427.
30. Smith K. S. (1979) An analytic nodal method for solving the two-group, multidimensional, static and transient neutron diffusion equations. Engineers Thesis, Department of Nuclear Engineering, M.I.T., Cambridge, MA, March.
31. Greenman G., Smith K. S. and Henry A. F. (1979) Recent advances in an analytic nodal method for static and transient reactor analysis. *The Topical Meeting on Computational Methods in Nuclear Engineering*, Vol. 1, pp. 3–49, Williamsburg, 23–25 April.
32. Gelbard E., Davis J. and Pearson J. (1959) Iterative Solutions to the P_L and Double-P_L Equations. *Nucl. Sci. Eng.* **5,** 36.
33. Smith K., Henry A. F. and Loretz R. A. (1980) The determination of homogenized diffusion theory parameters for coarse mesh nodal analysis. *Proceedings of the Conference on Advances in Reactor Physics and Shielding*, p. 294, Sun Valley, 14–19 September.
34. Borresen S. (1981) Experience, status and advanced applications of Presto. *International Topical Meeting on Advances in Mathematical Methods for the Solution of Nuclear Engineering Problems*, Vol. 1, p. 283, Munich, 27–29 April.
35. Ver Planck D. M. (1983) SIMULATE-E; A nodal core analysis program for light water reactors, NP 2792 CCM.
36. Rothleder B. M., *et al.* NODEP-2 Code Description, ARMP documentation, EPRI, to be published.
37. Hughes R. P. (1978) A unified derivation of the various definitions of lattice cell diffusion coefficients. *Nucl. Sci. Eng.* **67,** 85.
38. Pierini G. (1970) A consistent homogenization procedure to obtain few-group cell parameters. *Atomkernenergie* **34.**
39. Bonalumi R. A. (1978) A rigorous calculation of homogenized diffusion theory parameters. *Trans. Am. Nucl. Soc.* **30,** 247.
40. Pierini G. (1985) Generalized neutron diffusion model for homogenized non-symmetric slabs. *Proceedings of the International Meeting on Advances in Nuclear Engineering Computational Methods*, Vol. 2, p. 590, Knoxville, 9–11 April.
41. Chiang R.-T. and Dorning J. (1980) A homogenization theory for lattices with burnup and non-uniform loading. *Proceedings of the Conference on Advances in Reactor Physics and Shielding*, p. 309, Sun Valley, 14–19 September.
42. Chiang R.-T. (1982) A lattice homogenization theory for coarse mesh diffusion analysis. *Proceedings of the Topical Meeting on Advances in Reactor Physics and Core Thermal Hydraulics*, Vol. 1, p. 391, Kiamesha Lake, 22–24 September.
43. Worley B. A. and Henry A. F. (1977) Spatial homogenization of diffusion theory parameters, Department of Nuclear Engineering, Massachusetts Institute of Technology Report COO-2262-10, MITNE-210.
44. Henry A. F., *et al.* (1978) Spatial homogenization of diffusion theory parameters. *IAEA Technical Committee Meeting on Homogenization Methods in Reactor Physics*, Lugano, 13–15 November.
45. Koebke K. (1978) A new approach to homogenization and group condensation. *IAEA Technical Committee Meeting on Homogenization Methods in Reactor Physics*, Lugano, 13–15 November.
46. Koebke K. (1981) Advances in homogenization and dehomogenization. *International Topical Meeting on Advances in Mathematical Methods for the Solution of Nuclear Engineering Problems*, Vol. 2, p. 59, Munich, 27–29 April.
47. Wagner M. R. and Koebke K. (1983) Progress in nodal reactor analysis. *A Topical Meeting on Advances in Reactor Computations*, Vol. II, p. 941, Salt Lake City, 28–30 March.
48. Koebke K. (1985) Private communication.
49. Smith K. S. (1980) Spatial homogenization methods for light water reactors, Thesis, Department of Nuclear Engineering, Mass. Inst. of Tech., Cambridge, Ma.
50. Koebke K., Haase H., Hetzelt L. and Winter H. J. (1985) Application and verification of the simplified equivalence theory for burnup states. *Proceedings of the International Meeting on Advances in Nuclear Engineering Computational Methods*, Vol. 2, p. 607, Knoxville, 9–11 April.
51. Ver Planck D. M. (1985) Private communication.
52. Cheng A. Y., Henry A. F. and Hoxie C. L. (1981) A method for determining equivalent homogenized parameters. *International Topical Meeting on Advances in Mathematical Methods for the Solution of Nuclear Engineering Problems*, Vol. 2, p. 3, Munich, 27–29 April.

APPENDIX 1.1. SPECIFICATIONS FOR THE ONE-DIMENSIONAL PARTIALLY-POISONED-ASSEMBLY BENCHMARK PROBLEM

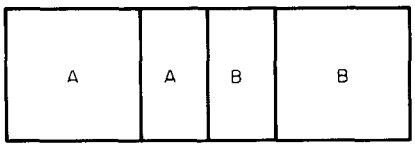

Composition	Group, g	D_g	Σ_{ag}	$\nu\Sigma_{fg}$	$\Sigma_{gg'}$
A	1	1.32000	0.00900	0.006	0.017
	2	0.38300	0.08000	0.104	0.0
B	1	1.32000	0.00900	0.006	0.017
	2	0.38300	0.09000	0.104	0.0

$X_1 = 1.0$, $X_2 = 0.0$.
Assembly pitch: 21.00 cm.
Boundary conditions: reflective: left, bottom, top, right.

APPENDIX 1.2. SPECIFICATIONS FOR THE ZION PWR BENCHMARK PROBLEM

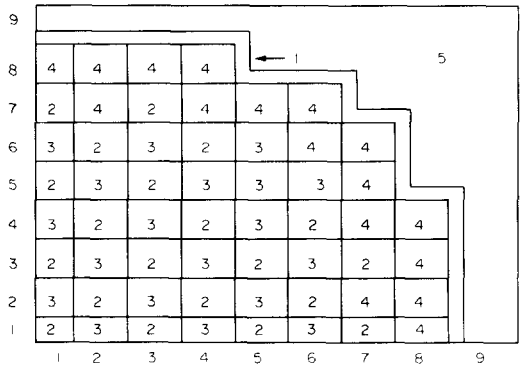

Composition	Group, g	D_g	Σ_{ag}	$\nu\Sigma_{fg}$	$\Sigma_{gg'}$
1	1	1.02130	0.00322	0.0	0.0
	2	0.33548	0.14596	0.0	0.0
2	1	1.47160	0.00855	0.00536	0.01742
	2	0.37335	0.06669	0.10433	0.0
3	1	1.41920	0.00882	0.00601	0.01694
	2	0.37370	0.07606	0.12472	0.0
4	1	1.42650	0.00902	0.00653	0.01658
	2	0.37424	0.08359	0.14120	0.0
5	1	1.45540	0.00047	0.0	0.02903
	2	0.28994	0.00949	0.0	0.0

$X_1 = 1.0$, $X_2 = 0.0$.
Assembly pitch: 21.608 cm. Baffle thickness: 2.8575 cm.
Boundary condtions: reflective: left, bottom, zero flux: top, right.
$\Sigma_{tr,g} = 1/3D_g$ for isotropic scattering, transport problem.

APPENDIX 1.3. SPECIFICATIONS FOR THE DVP BWR BENCHMARK PROBLEM

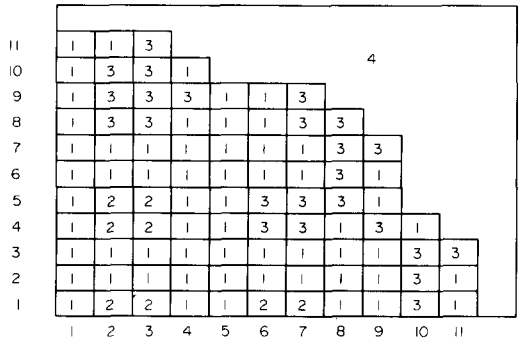

Composition	Group, g	D_g	Σ_{ag}	$\nu\Sigma_{fg}$	$\Sigma_{gg'}$
1	1	1.62020	0.00654	0.00415	0.01462
	2	0.48403	0.04850	0.06099	0.0
2	1	1.40100	0.00944	0.00437	0.01798
	2	0.39056	0.06661	0.07142	0.0
3	1	1.38370	0.00696	0.00437	0.02030
	2	0.37643	0.05106	0.06330	0.0
4	1	1.41240	0.000038	0.0	0.04575
	2	0.24434	0.01031	0.0	0.0

Composition	$ADF_{1\ wide}$	$ADF_{2\ wide}$	$ADF_{1\ narrow}$	$ADF_{2\ narrow}$
1	0.9288	1.6570	0.9966	1.1332
2	0.8423	0.6809	1.0787	1.6423
3	0.9114	1.5805	0.9989	1.1664

$X_1 = 1.0$, $X_2 = 0.0$.
Assembly pitch: 15.313 cm.
Boundary conditions: reflective: left, bottom, zero flux: top, right.

APPENDIX 1.4. SPECIFICATIONS FOR THE HAFAS BWR BENCHMARK PROBLEM

Quadrant of the two-dimensional Reactor

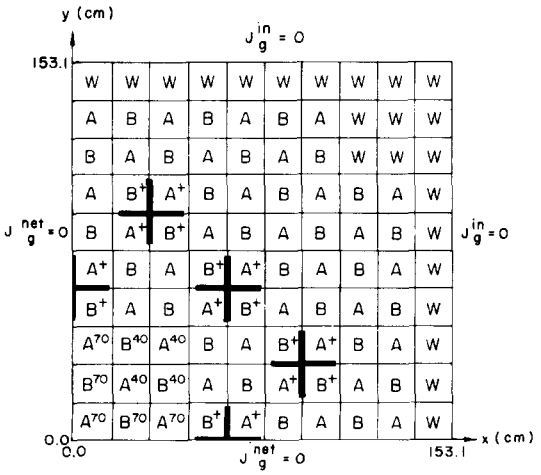

Fuel Assembly Description

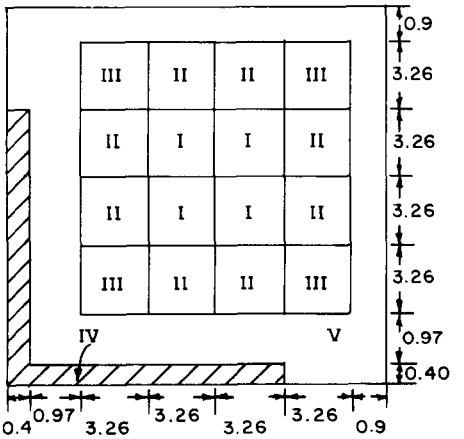

Composition-to-Zone Assignments

Zone	Assembly Type								
	A	A^{40}	A^{70}	A^{+}	B	B^{40}	B^{70}	B^{+}	W
I	1	5	9	1	2	6	10	2	15
II	2	6	10	2	3	7	11	3	15
III	3	7	11	3	4	8	12	4	15
IV	13	13	13	14	13	13	13	14	15
V	13	13	13	13	13	13	13	13	15

Cross sections

Composition	D_1	Σ_{aa1}	$\nu\Sigma_{f_1}$	$\Sigma_{1\to 2}$	D_2	Σ_{a2}	$\nu\Sigma_{f_2}$
1	1.400	0.0090	0.0065	0.0160	0.375	0.080	0.1220
2	1.400	0.0090	0.0057	0.0170	0.375	0.070	0.1000
3	1.400	0.0090	0.0051	0.0180	0.375	0.060	0.0800
4	1.400	0.0090	0.0051	0.0180	0.375	0.050	0.0700
5	1.680	0.0080	0.0063	0.0100	0.530	0.077	0.1180
6	1.680	0.0085	0.0055	0.0105	0.530	0.067	0.0960
7	1.680	0.0090	0.0049	0.0110	0.530	0.057	0.0780
8	1.680	0.0090	0.0049	0.0110	0.530	0.047	0.0680
9	2.000	0.0078	0.0061	0.0052	0.800	0.073	0.1140
10	2.000	0.0082	0.0053	0.0053	0.800	0.063	0.0920
11	2.000	0.0086	0.0047	0.0054	0.800	0.053	0.0720
12	2.000	0.0086	0.0047	0.0054	0.800	0.043	0.0620
13	1.530	0.0005	0.0	0.0310	0.295	0.009	0.0
14	1.110	0.08375	0.0	0.00375	0.185	0.950	0.0
15	2.000	0.0	0.0	0.0400	0.300	0.010	0.0

$\chi_1 = 1.0$, $\chi_2 = 0.0$, $\nu = 2.5$.
Boundary conditions: reflective: left, bottom, zero incoming flux: top, right.
$\Sigma_{tr,g} = 1/3D_g$ for isotropic scattering, transport problem.